Haupt/Masterstudiengang Physik
Methoden moderner Röntgenphysik II:
Streuung und Abbildung
SS 2013

Biology III: Experiments / Refinement

Thomas R. Schneider, EMBL Hamburg
27/6/2013
thomas.schneider@embl-hamburg.de

EMBL

Recap

- Phasing methods
  - Ab initio
  - Molecular Replacement – 25%. Model bias
  - Multiple Isomorphous Replacement
  - Multiple Anomalous Diffraction
  - Single Anomalous Diffraction – 1%. phase ambiguity
- Importance of accurate measures of data quality

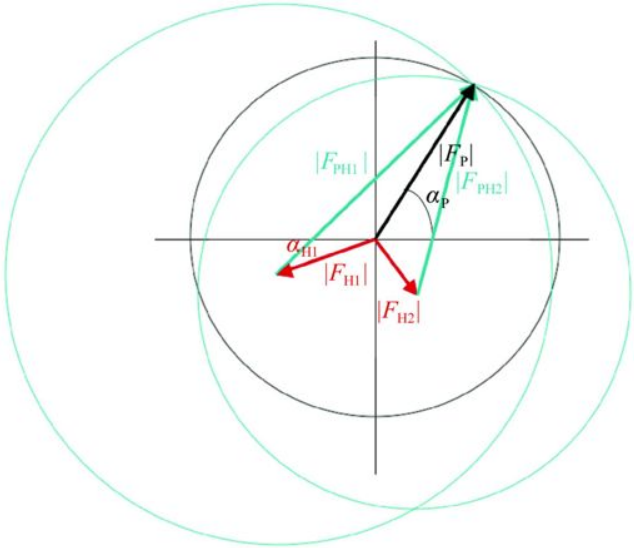

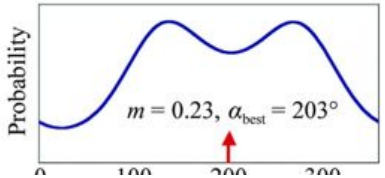

$$\left|F_{hkl}\right| \neq \left|F_{\overline{hkl}}\right|$$

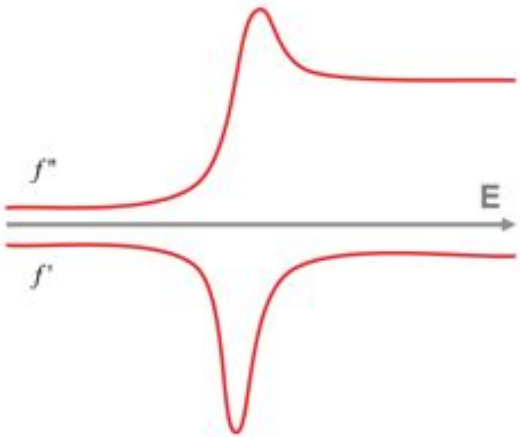

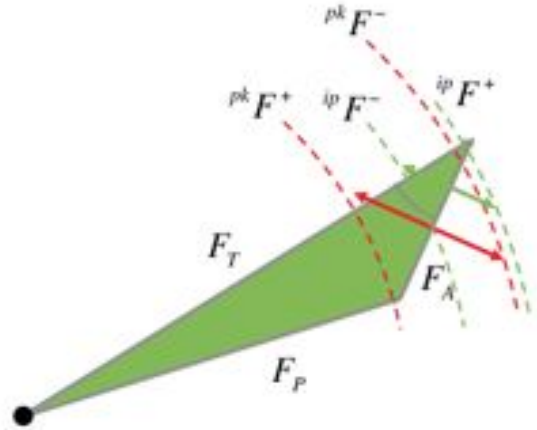

Today

- Experiments
  - Beams
  - Diffractometry
  - Low-energy data collection
  - Automation
- Refinement
- XFEL

Diffraction angles and resolution

- Smaller lattice spacings *d* give rise to higher diffraction angles *Θ*:

$$2\, d \sin\Theta = n\, \lambda$$

$$\Theta = \arcsin(n\, \lambda / 2d)$$

$$\arcsin (1\ \text{Å} / 2 * 3\ \text{Å}) = 9.6^\circ$$
$$\arcsin (1\ \text{Å} / 2 * 1\ \text{Å}) = 30.0^\circ$$

- The lattice spacing roughly corresponds to the optical resolution.
- The higher the diffraction angle, the weaker is the average diffracted intensity

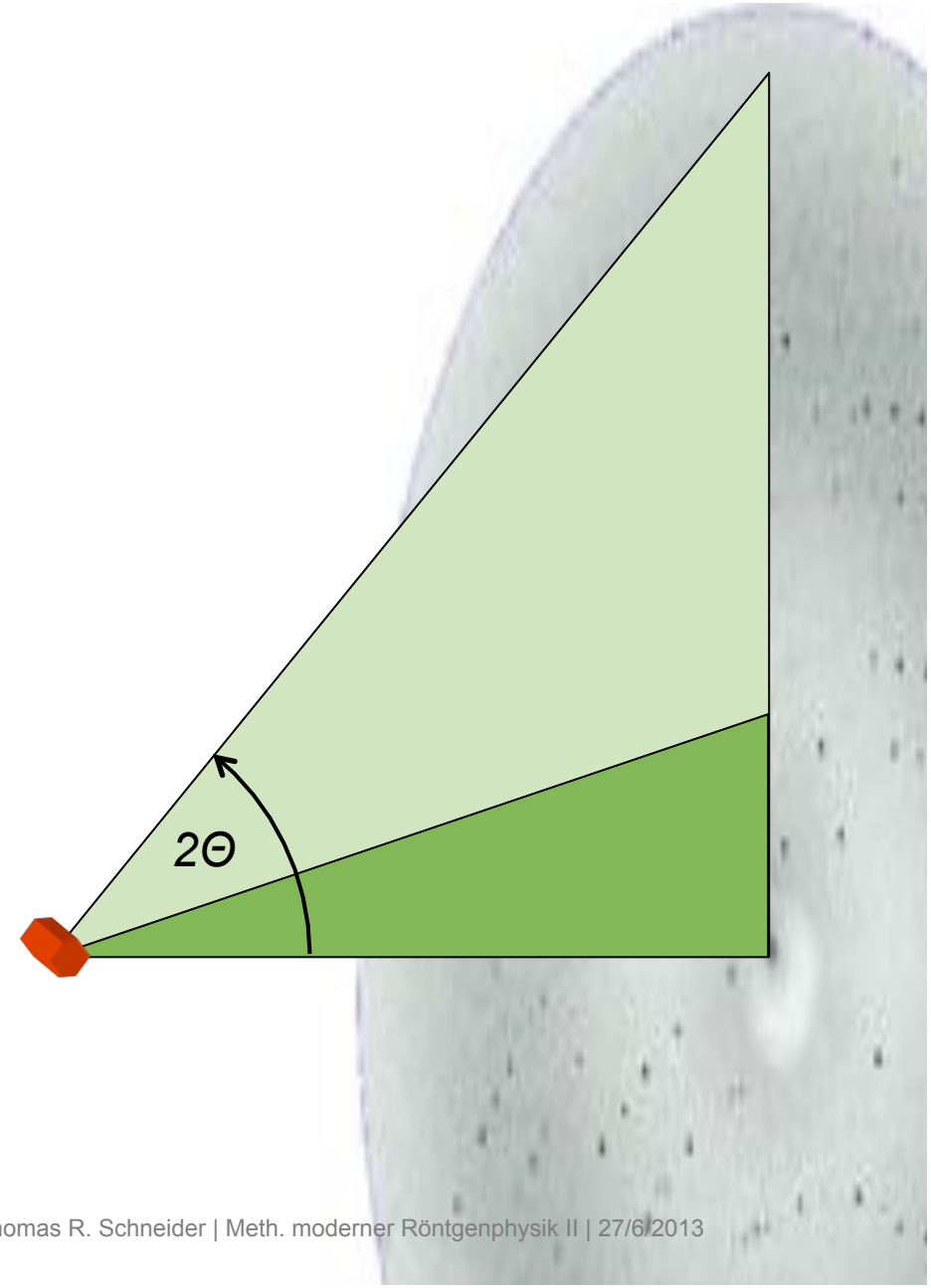

Limited resolution in crystallography

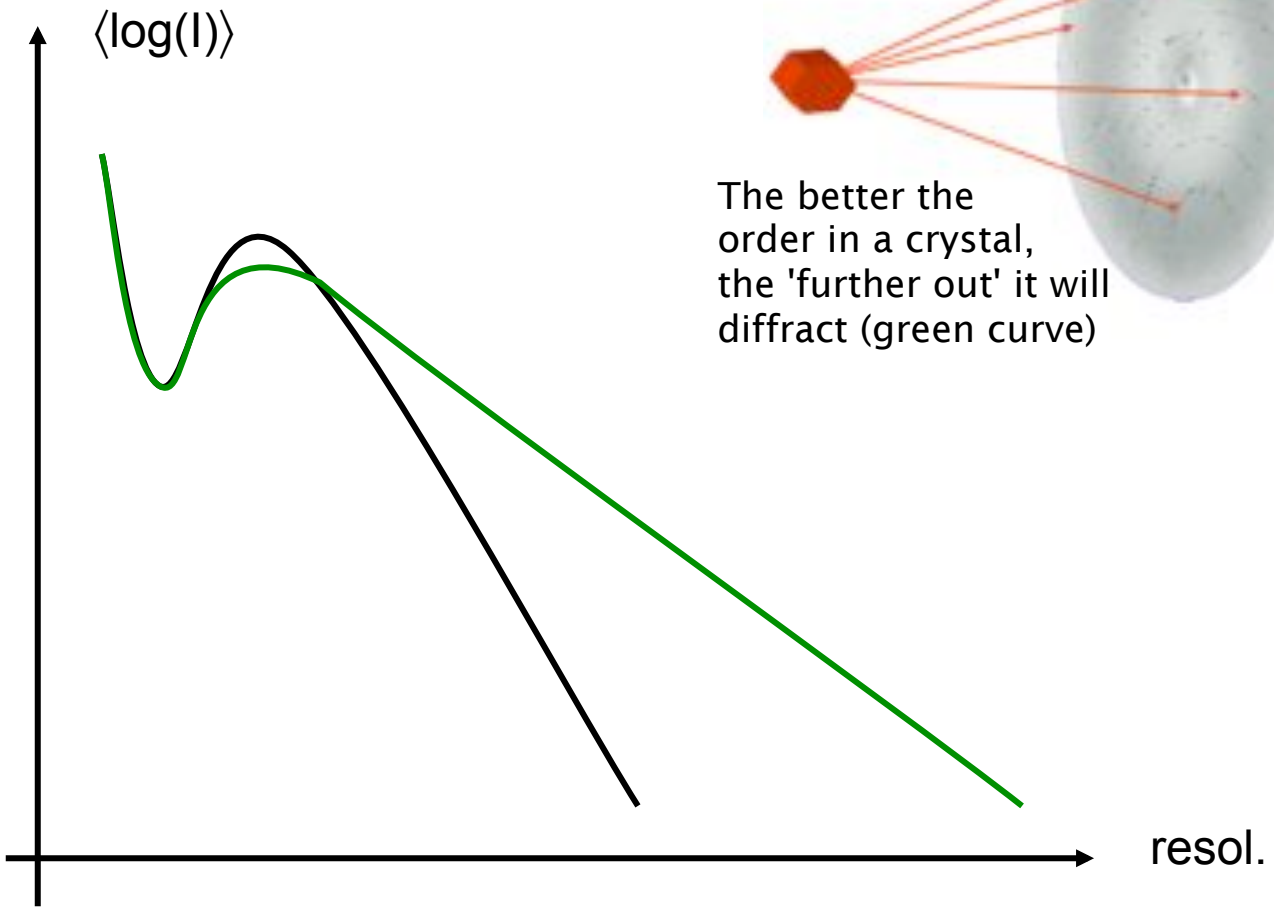

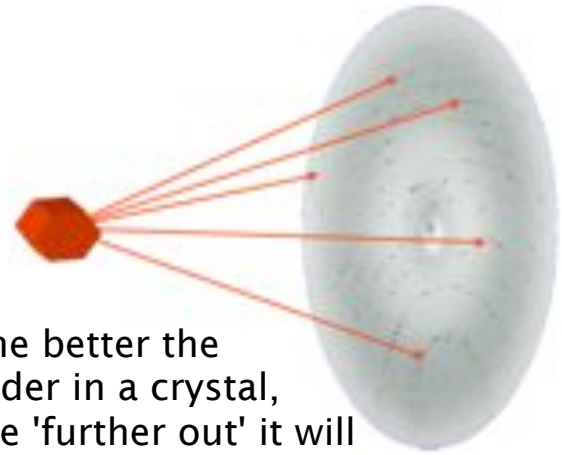

The better the order in a crystal, the 'further out' it will diffract (green curve)

- Diffraction data have an enormous dynamic range
- The higher the resolution / the larger the unit cell, the smaller the diffracted intensities

Limited resolution in crystallography

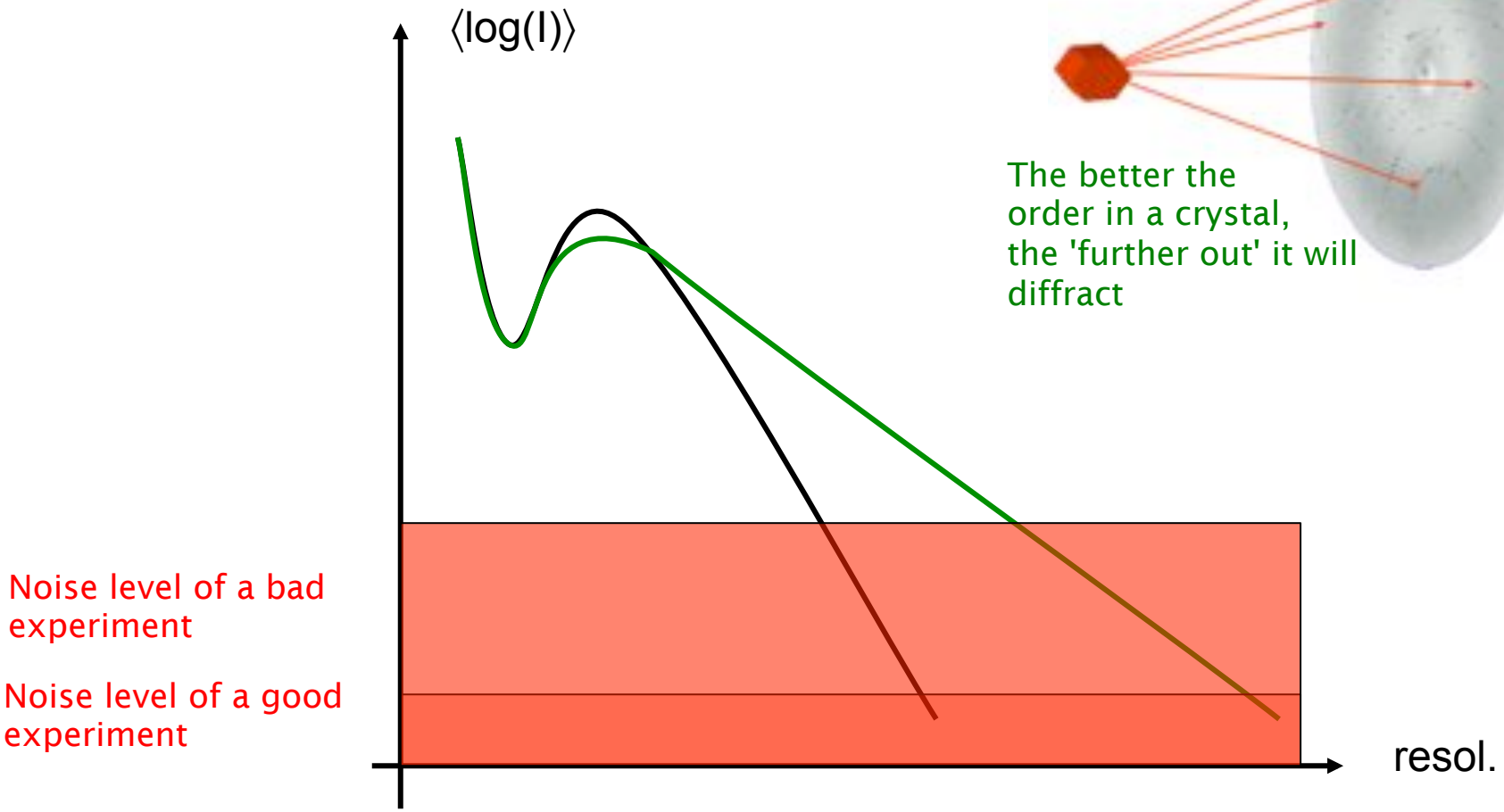

- Diffraction data have an enormous dynamic range
- The higher the resolution / the larger the unit cell, the smaller the diffracted intensities

Why does anomalous phasing not work all the time?

- Molecule of interest does not contain anomalous scatterers
  - Seleno-Met incorporation
  - Derivatization
  - Co-crystallization
- The signal is too weak (small differences between large numbers)
  - Increase signal by choosing the right wavelength (synchrotron ...)
  - Enhance signal e.g. by oxidation of Se-atoms
  - Decrease background by optimizing the hardware, crystal mount, experiment
  - Add extra data -> SIRAS, MIRAS
  - More / more accurate data (inverse beam, kappa geometry)
- Crystals suffer from radiation damage
  - Keep crystal at cryogenic temperatures
  - Play tricks prolonging crystal lifetime (scavengers)
  - Careful use of tolerable dose (-> BEST)
  - Data from several positions on the same crystal
  - Data from several crystals

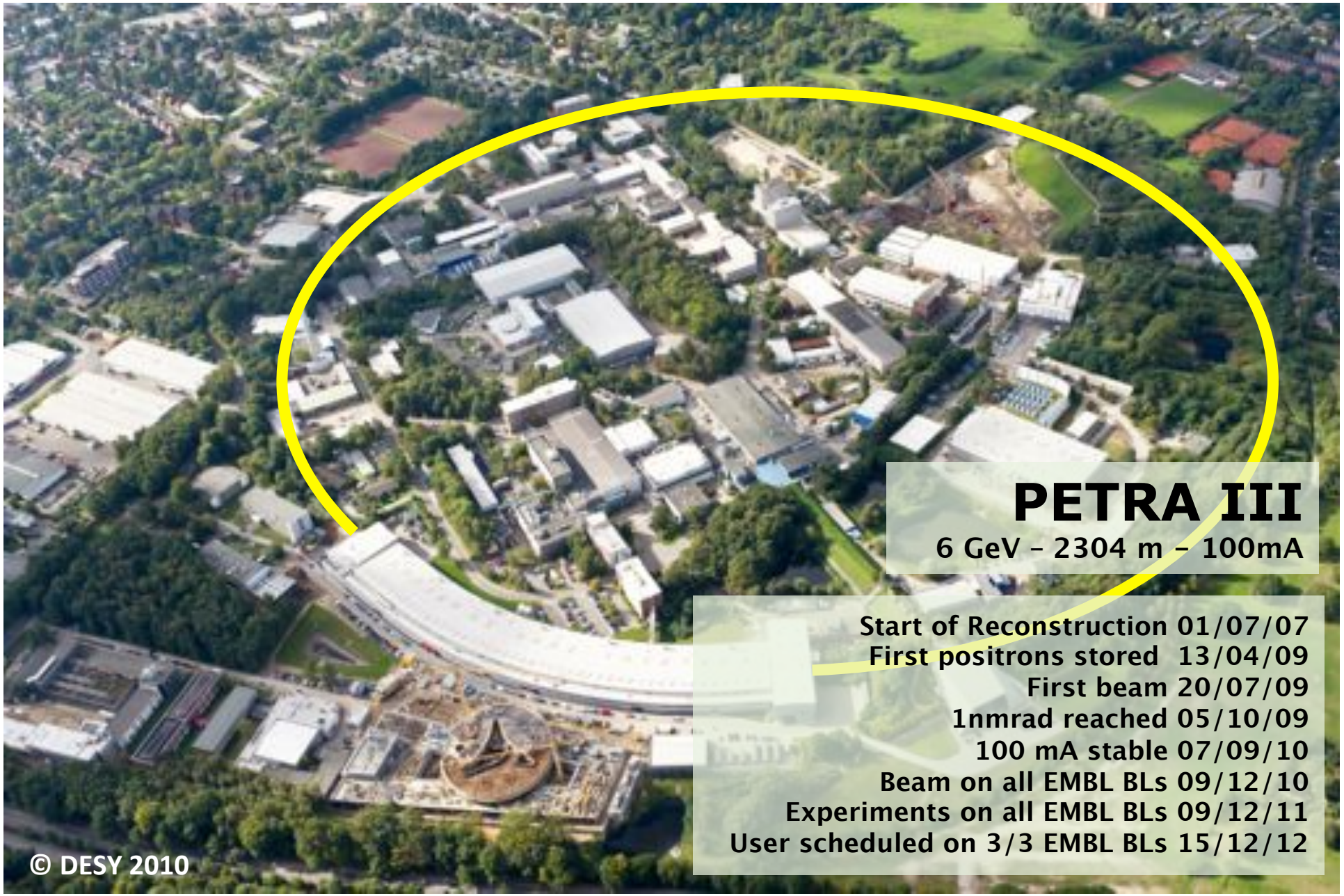
PETRA III
6 GeV – 2304 m – 100mA
Start of Reconstruction 01/07/07
First positrons stored 13/04/09
First beam 20/07/09
1nmrad reached 05/10/09
100 mA stable 07/09/10
Beam on all EMBL BLs 09/12/10
Experiments on all EMBL BLs 09/12/11
User scheduled on 3/3 EMBL BLs 15/12/12
© DESY 2010


© DESY 2010

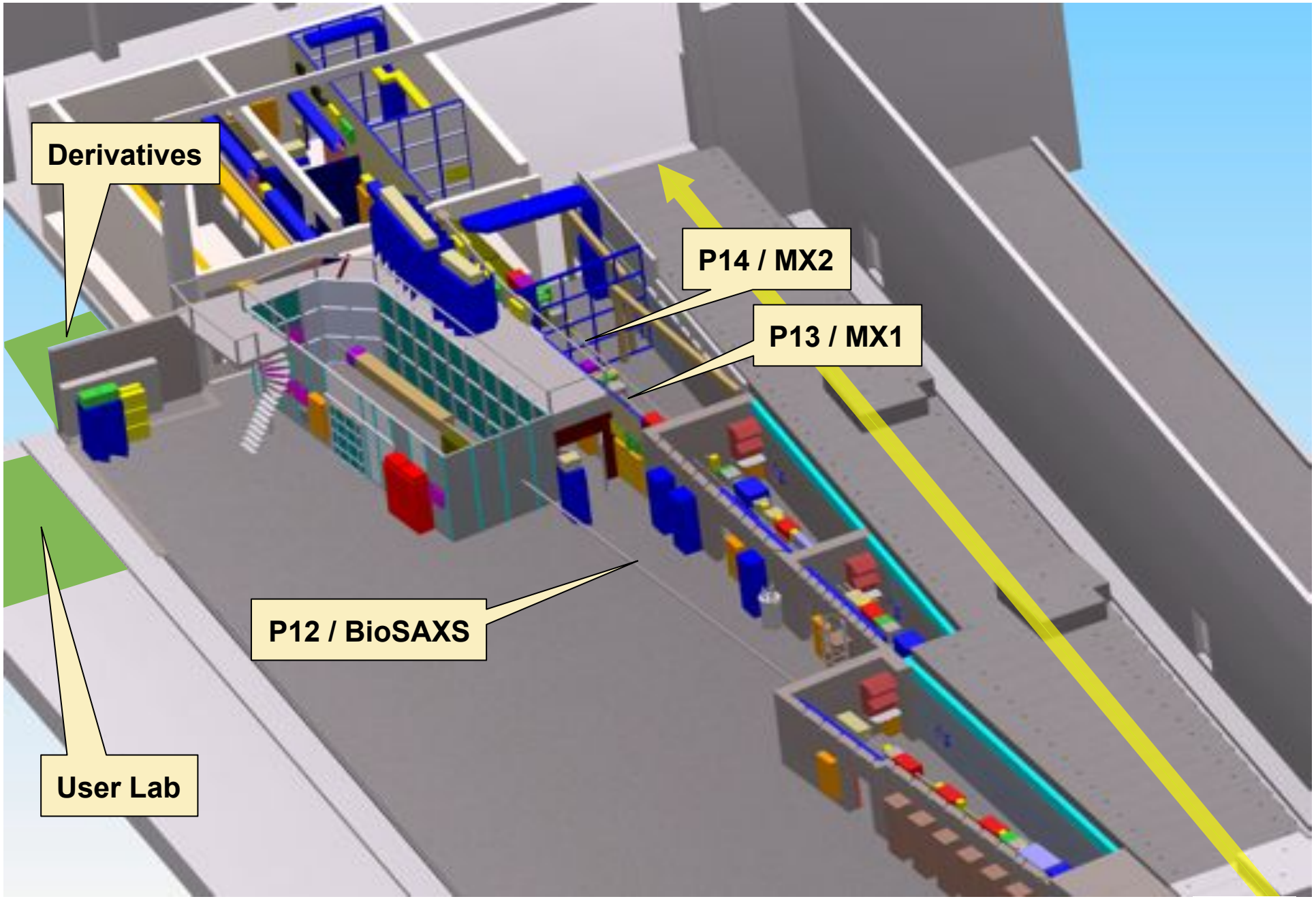
Derivatives
P14 / MX2
P13 / MX1
P12 / BioSAXS
User Lab

EMBL@PETRA3 - Optics

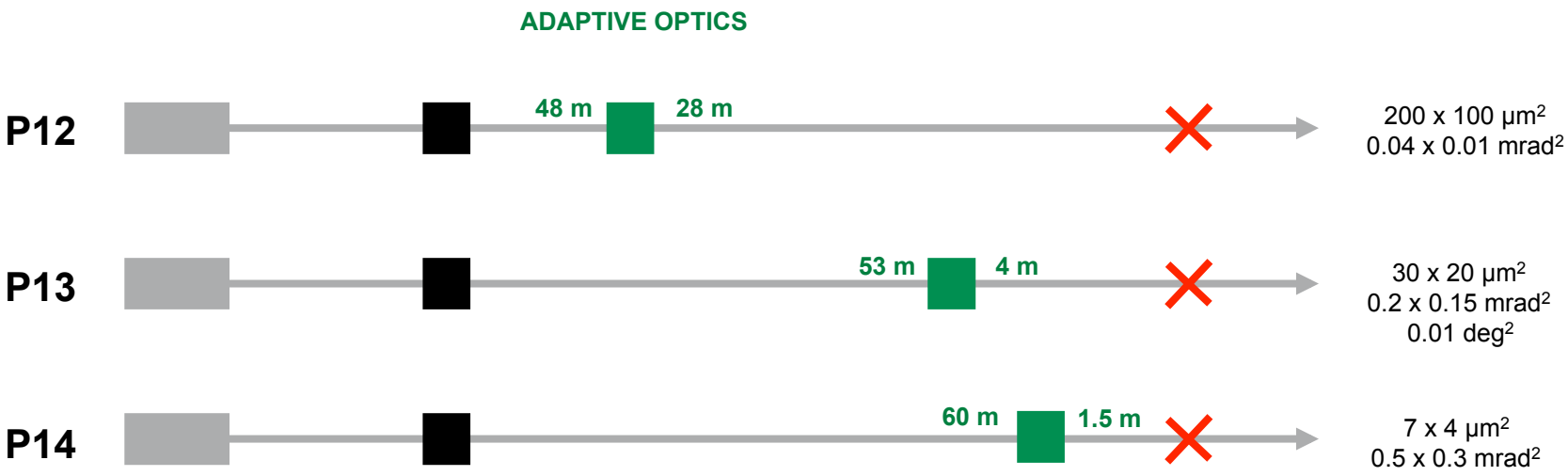

	P12:BioSAXS	P13:MX1	P14:MX2
Energy [keV]	4–20	5(4)–17	7–35
Monochromators	Si(111)	Si(111)	Si(111)
Beam size H x V [μm²]	200 x 60	28 x 13	4 x 1
Divergence H x V [mrad]	0.04 x 0.01	0.2 x 0.15	<0.5 x <0.3
Demagnification H / V	1:1.4 / 1: 1.2	1:12 / 1:15	1:60 / 1:40
Intensity [ph/sec]	10^{13}	10^{13}	10^{12}

P13 / MX1

4-16keV, 30 µm focus

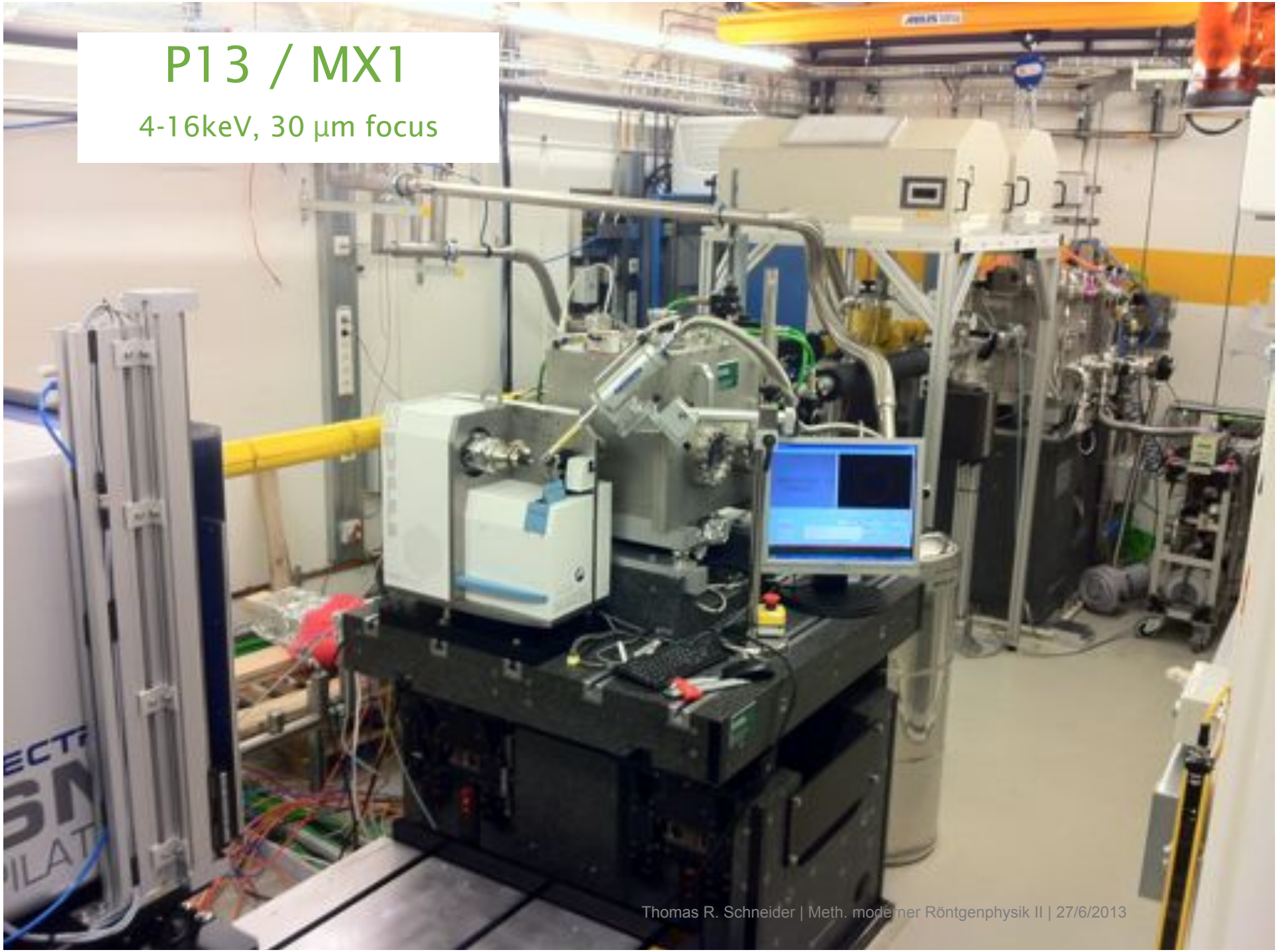

P14 / MX2

7-15 [35] keV, 5 x 7 [1x5] μm focus

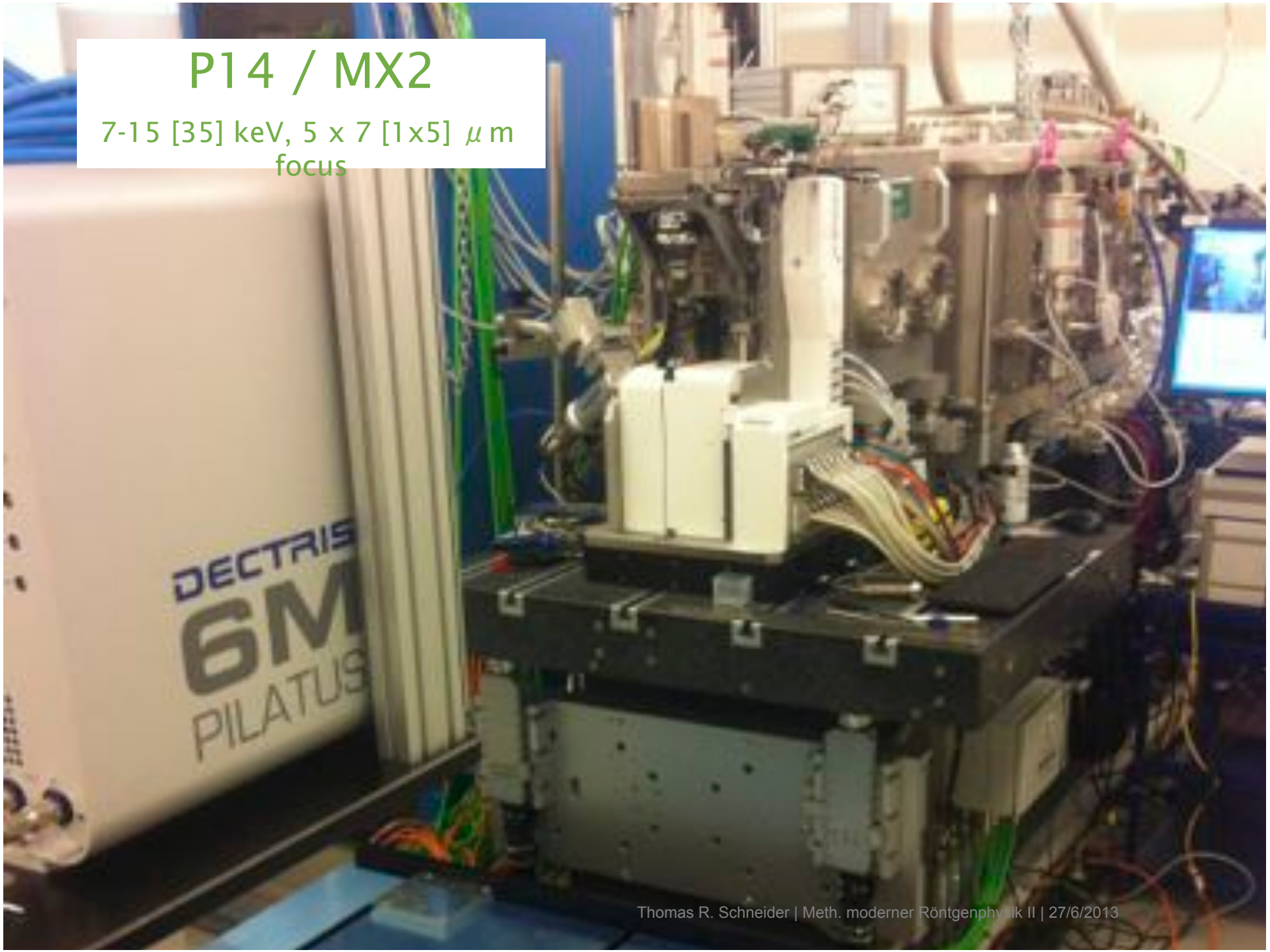

1 nmrad emmittance

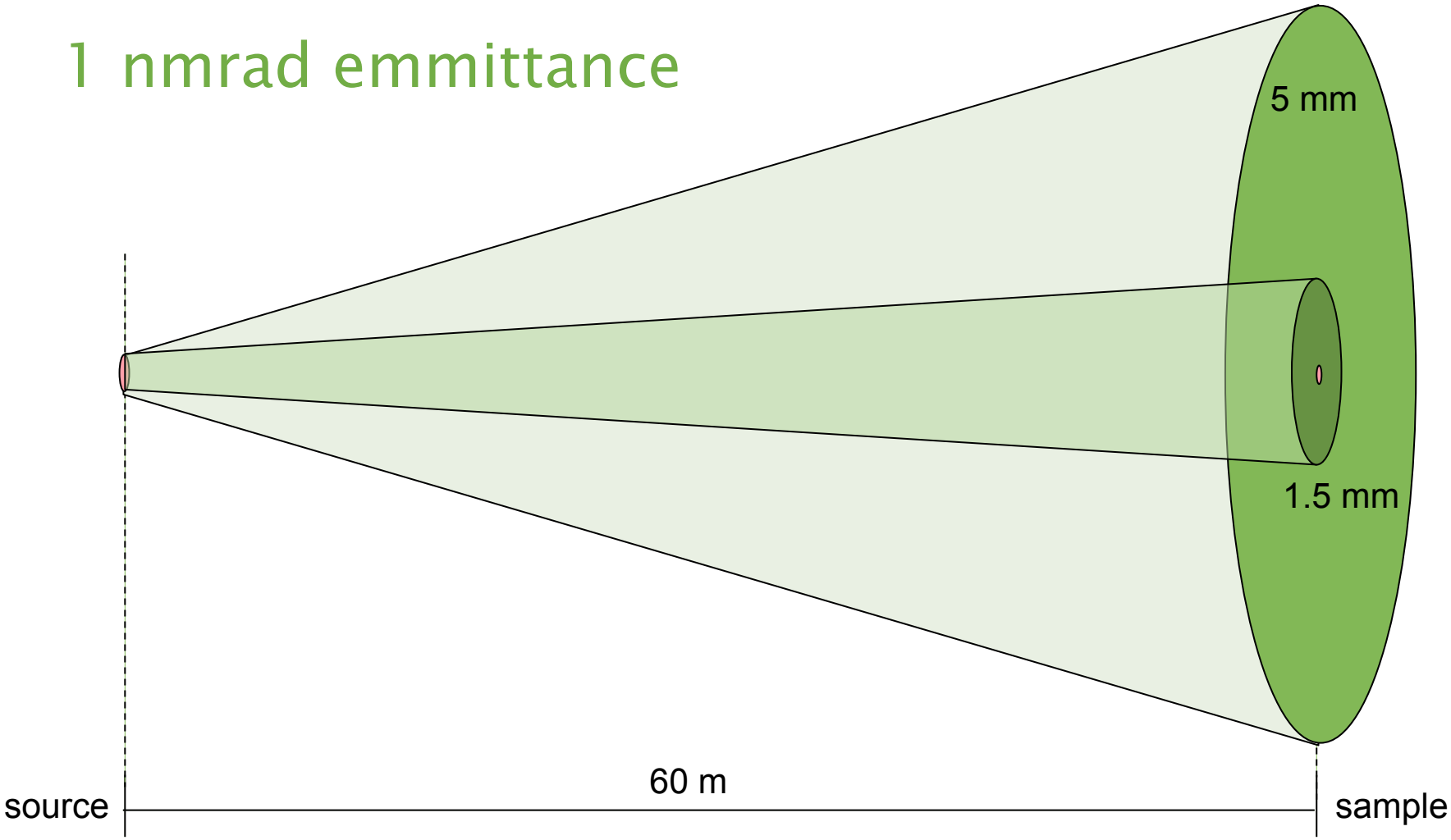

- 10^{13} monochromatic ph/sec to start with
- Flux through a 150 µm aperture is ca. 5 x 10^{11} ph/sec ⇒ 20 min. xtal-lifetime
- 20 µrad = 20 µm/m. Compare to 0.1° mos. = 1700 µrad

P14: unfocused beam

- Central beam profile is essentially top-hat
- flux: 5 x 10^{11} ph/sec in 150 µm ∅
- Beam positition is very stable:
  - rmsd 1.5 µm @ <10 Hz
  - rmsd 7 µm @ > 30 Hz
  - N.B. 60 m from the source, 16m from the DCM

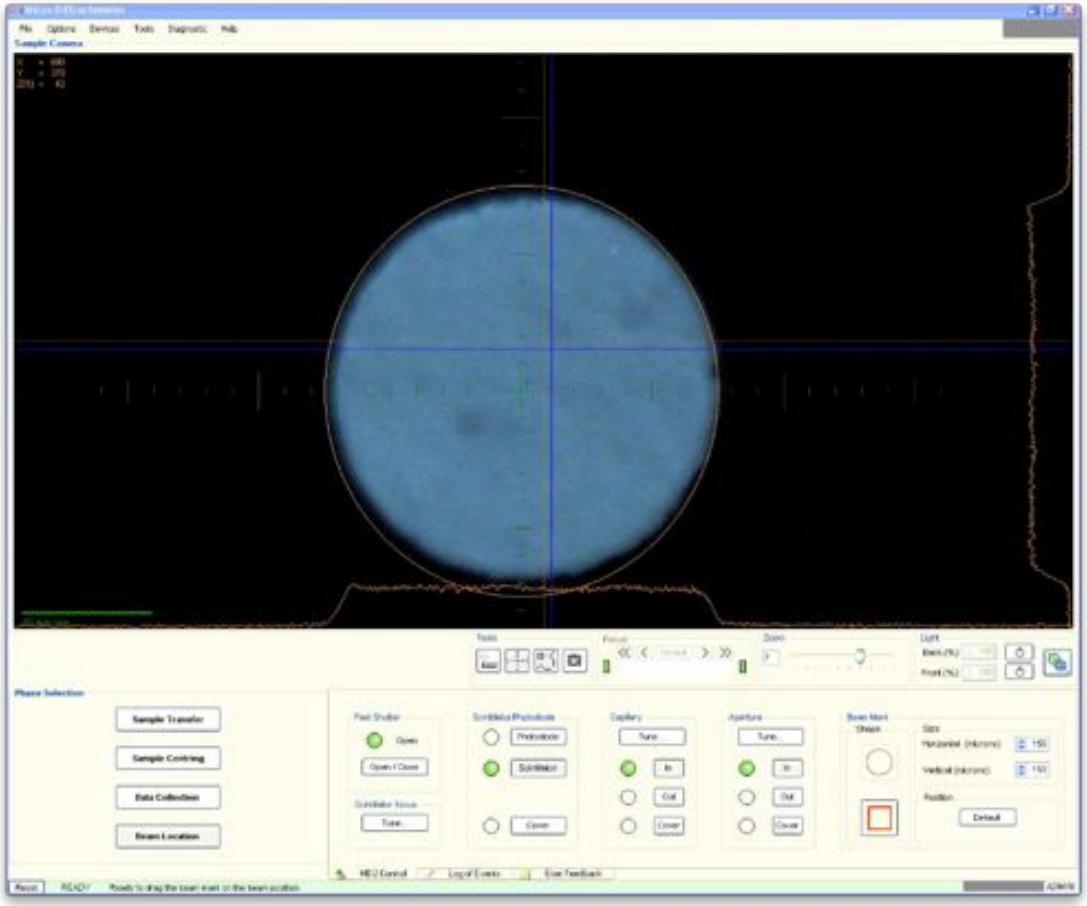

- Introduce vertically focusing mirror to reduce beam size from 1000 µm to 5 µm

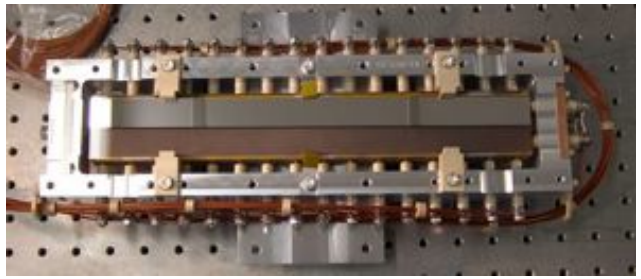

Vertical (Un)focusing …

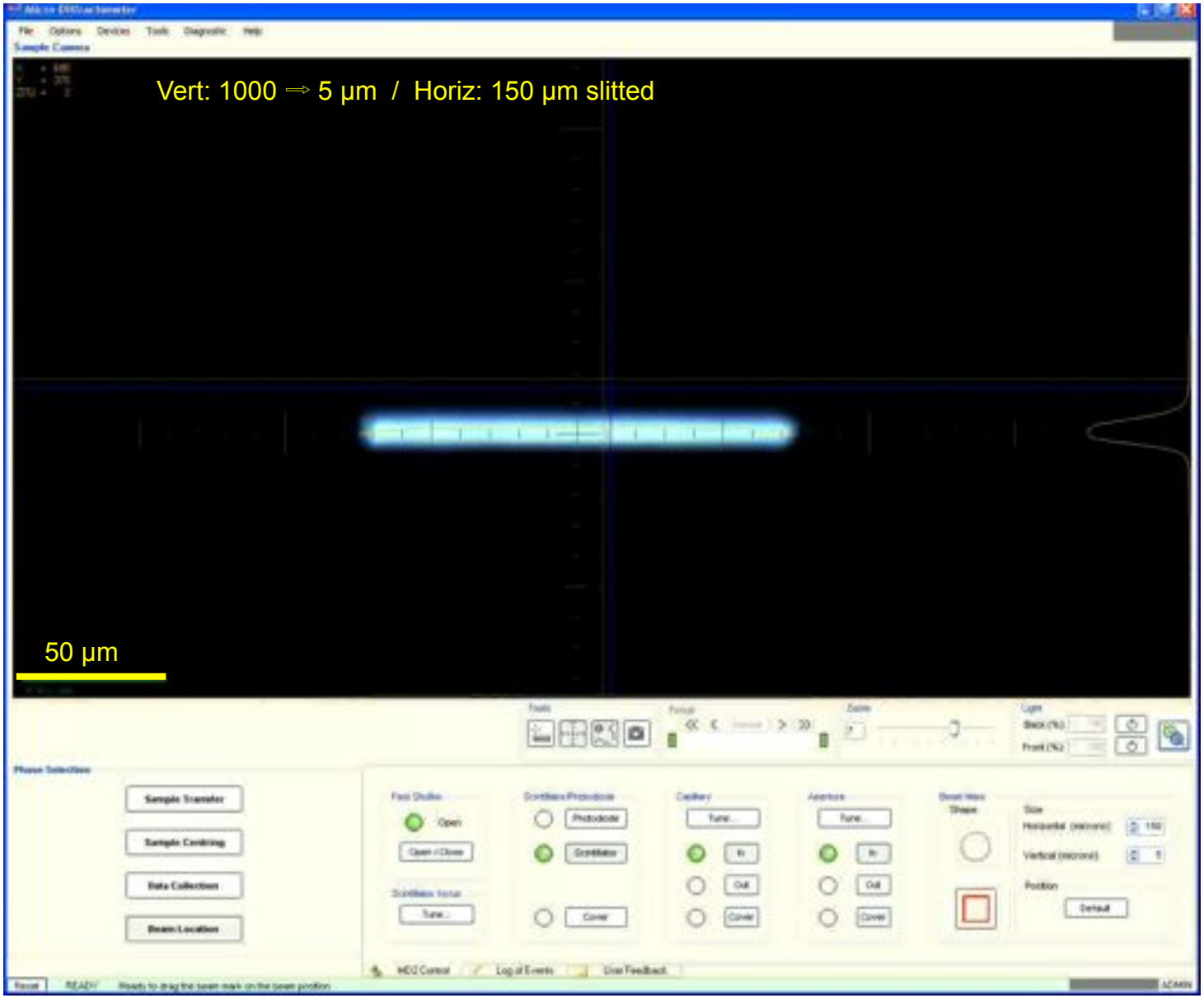

Adaptive X-ray focusing Mirrors

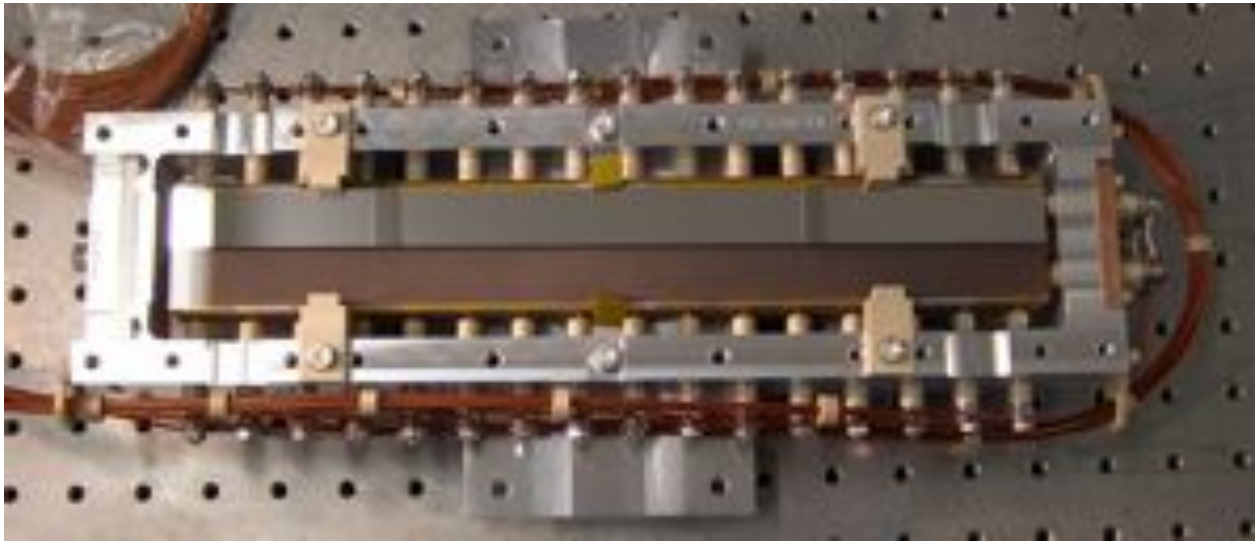

SESO bimorph mirror

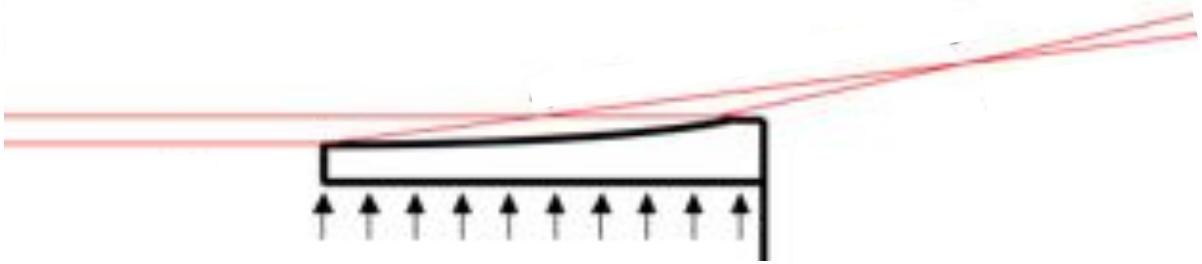

P14: horizontal focusing (11/12/12)

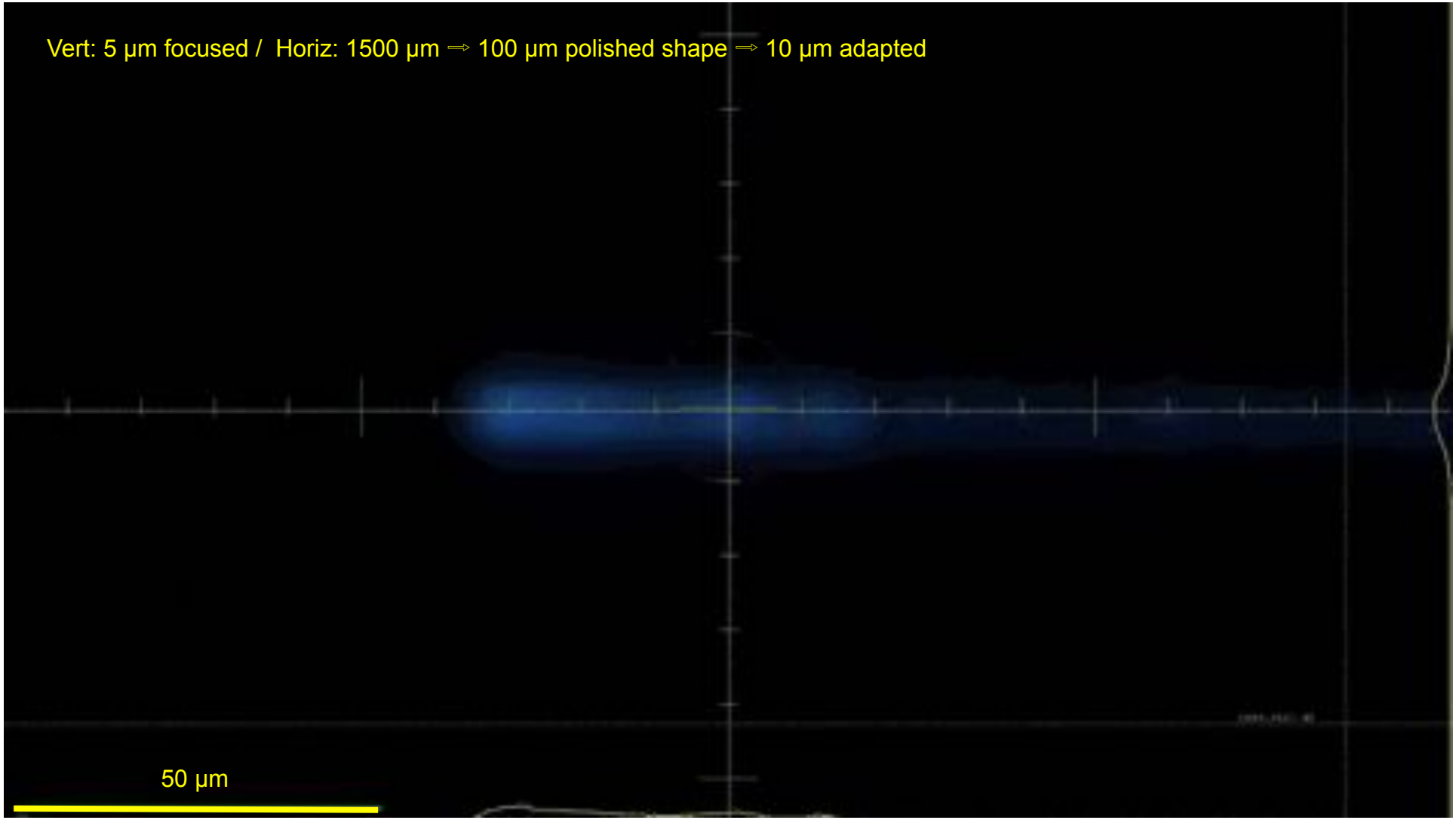

- 10^{12} ph/sec into 7 x 4 μm^2

P13: Focused beam I and II

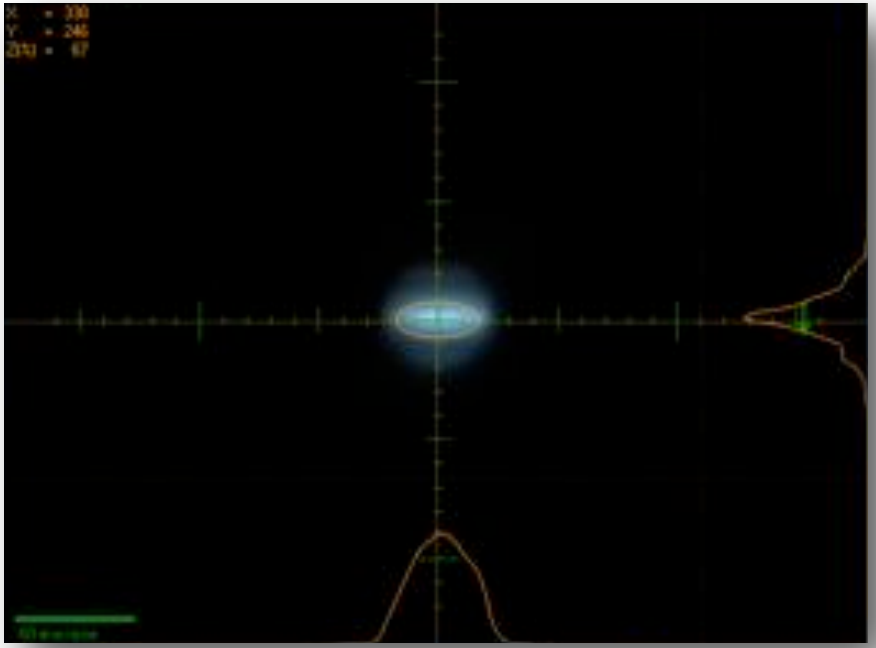

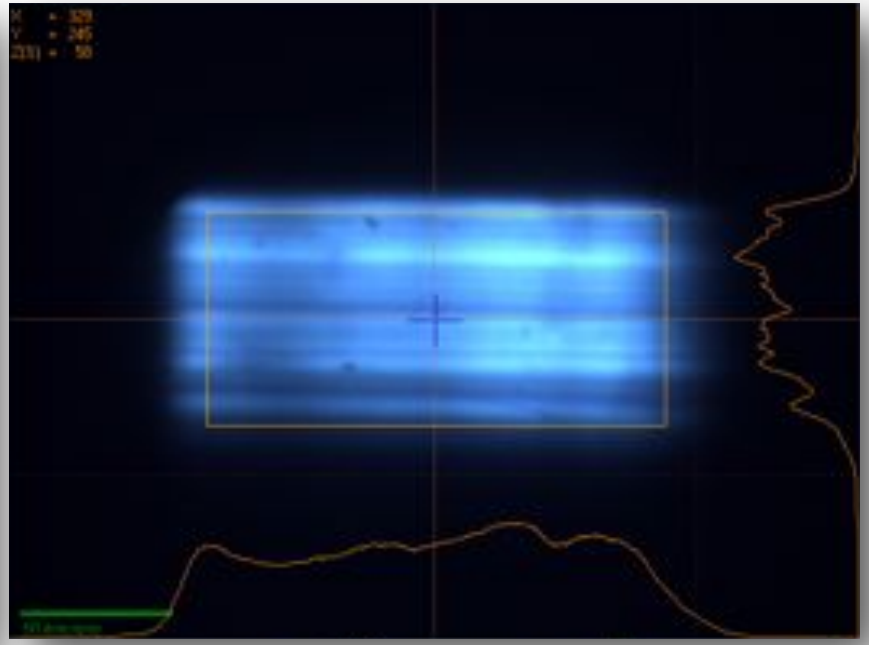

- H x V (FWHM) = 35 x 15 μm^2

- Focused, but detuned
- Shaped with Attocube-slits
- H x V (FVHM) = 150 x 70 μm^2

P13: Focused large beam, ConA [5/2/13]

- Concanavalin A crystal ~ $(50\ \mu m)^3$
- I222, 61.8 Å, 85.1 Å, 89.0 Å, 90˚, 90˚, 90˚
- E = 15 keV, λ = 0.827 Å, 3 x 10^{12} ph/sec (no att.)
- 1600 frames @ 0.05 sec / 0.1˚ = 160˚ in 80 sec

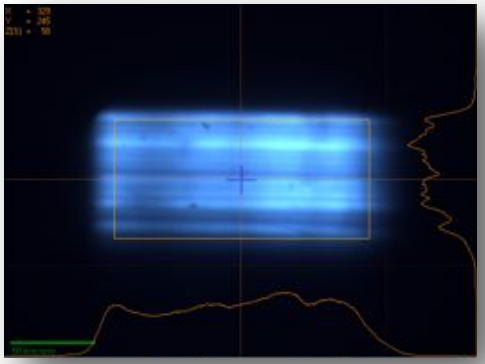

SUBSET OF INTENSITY DATA WITH SIGNAL/NOISE >= -3.0 AS FUNCTION OF RESOLUTION

RESOLUTION LIMIT	NUMBER OF REFLECTIONS OBSERVED	UNIQUE	POSSIB	COMPL OF DATA	R-FACTOR observed	R-FACTOR expected	I/SIGMA	R-meas	CC(1/2)	Anomal	SigAno Corr	Nano
5.08	5743	1858	1876	99.0%	1.8%	1.8%	52.99	2.2%	99.9*	24*	0.974	718
3.60	10368	3354	3373	99.4%	1.9%	2.0%	47.48	2.3%	99.9*	11*	0.900	1432
2.94	13992	4371	4394	99.5%	2.8%	2.7%	35.16	3.3%	99.9*	7	0.853	1965
2.54	15771	5159	5186	99.5%	4.5%	4.6%	21.05	5.5%	99.7*	-2	0.793	2262
2.28	18306	5829	5874	99.2%	7.0%	7.0%	14.39	8.4%	99.4*	12*	0.849	2633
2.08	20072	6463	6488	99.6%	9.2%	9.6%	10.54	11.1%	99.0*	1	0.782	2886
1.92	21413	7019	7080	99.1%	13.7%	13.7%	7.27	16.6%	98.4*	2	0.808	3077
1.80	23807	7521	7582	99.2%	25.5%	25.1%	4.26	30.7%	93.9*	-1	0.795	3416
1.70	23621	7833	8113	96.5%	46.2%	44.9%	2.39	56.0%	78.7*	2	0.784	3386
total	153093	49407	49966	98.9%	5.0%	5.0%	15.66	6.1%	99.9*	3	0.818	21775

Diffractometry

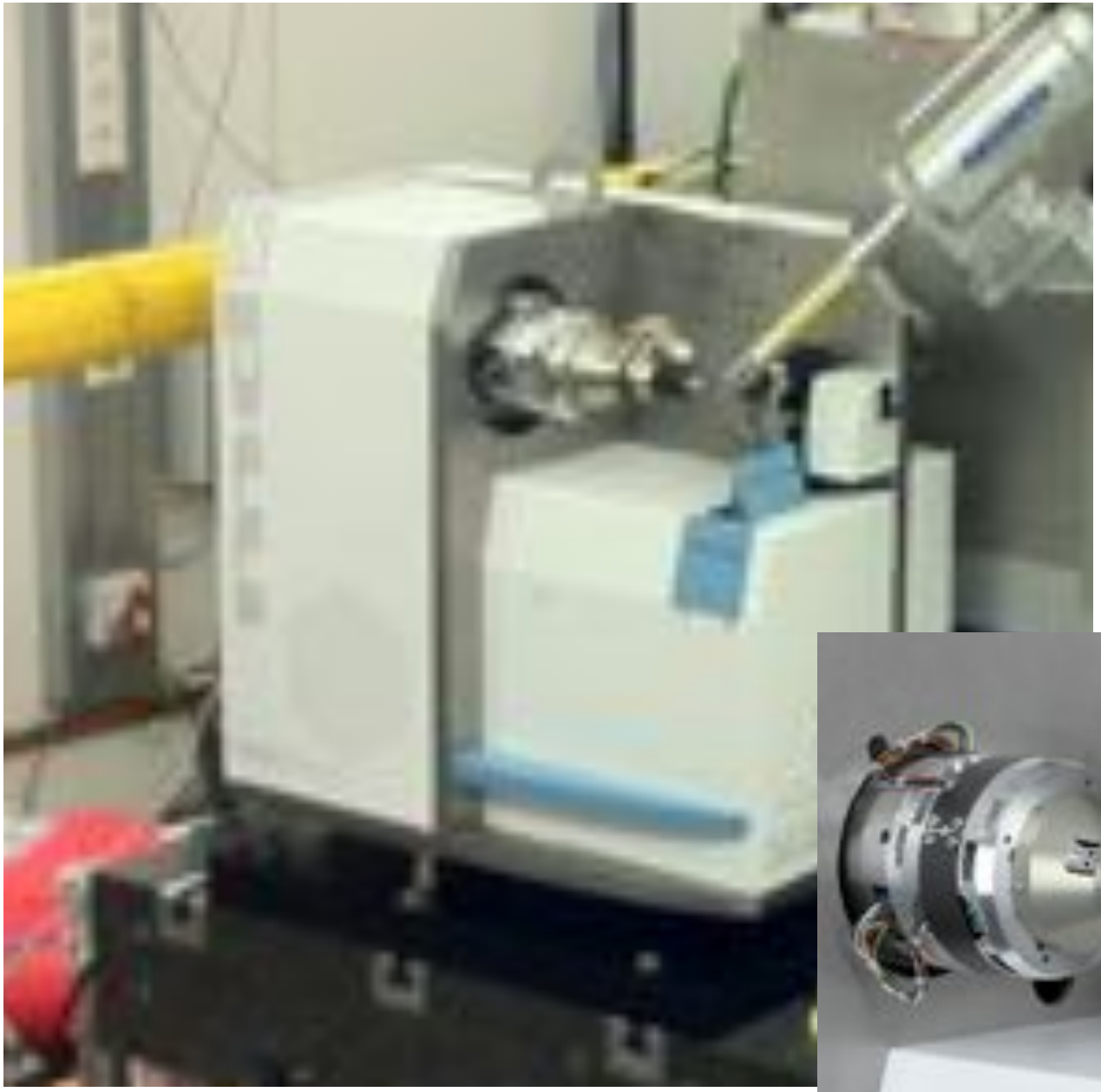

MD2 – measured sample run out

Sample vs spindle position (video microscope + image processing), 1 Turn w/o Kappa

Black line – average of multiple measurements (varying conditions)
Red lines – synchronous model

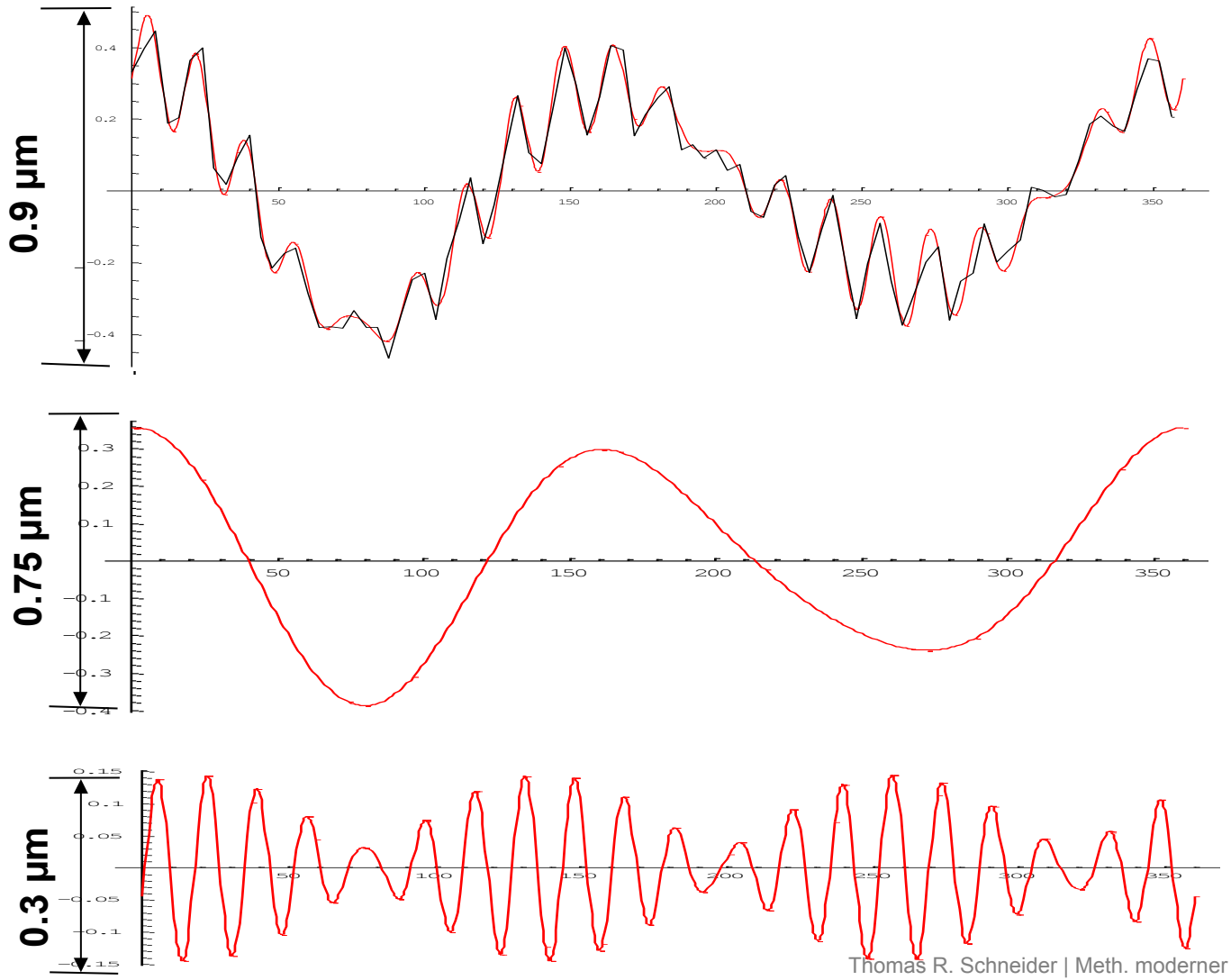

r.m.s.d. = 0.25 µm

peak-to-peak diameter = 0.9 µm

2nd (+3rd) harmonic
Gravity effect on the centering table

2.5 µm with Kappa

20th (+23rd) harmonic
Poles of the OMEGA motor

Vertical Diffractometry

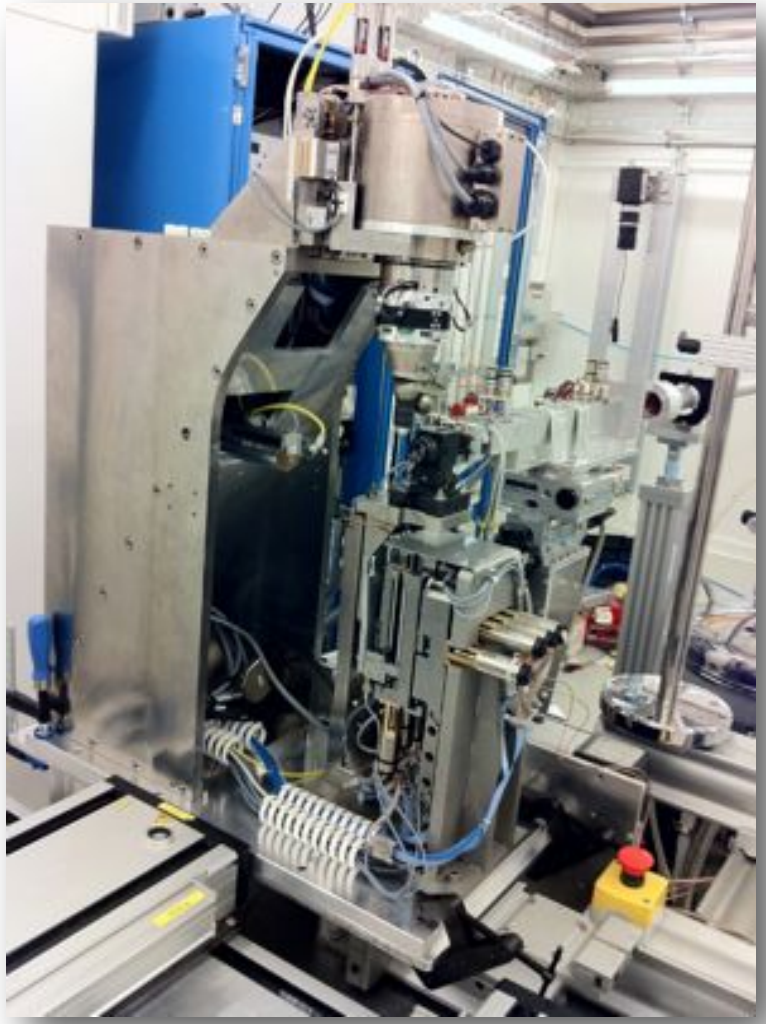

HPGonioV – summer 2011

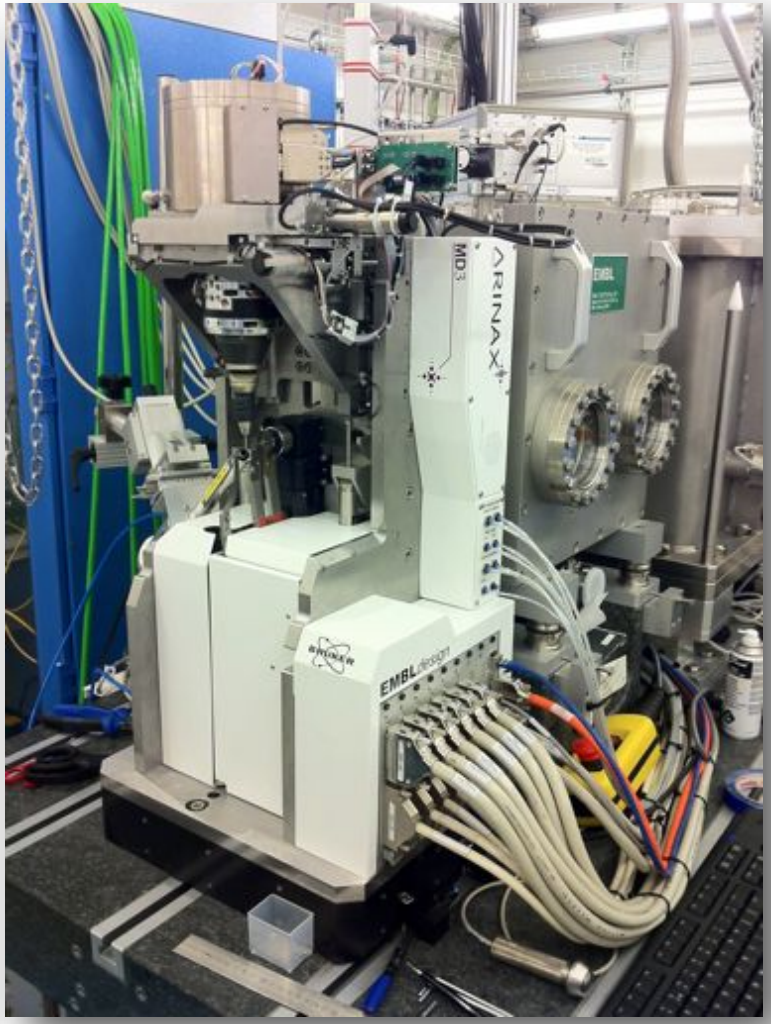

MD3 – 30/10/2012

'4D-Scan' (Florent Cipriani, Alexandre Gobbo, EMBL-GR)

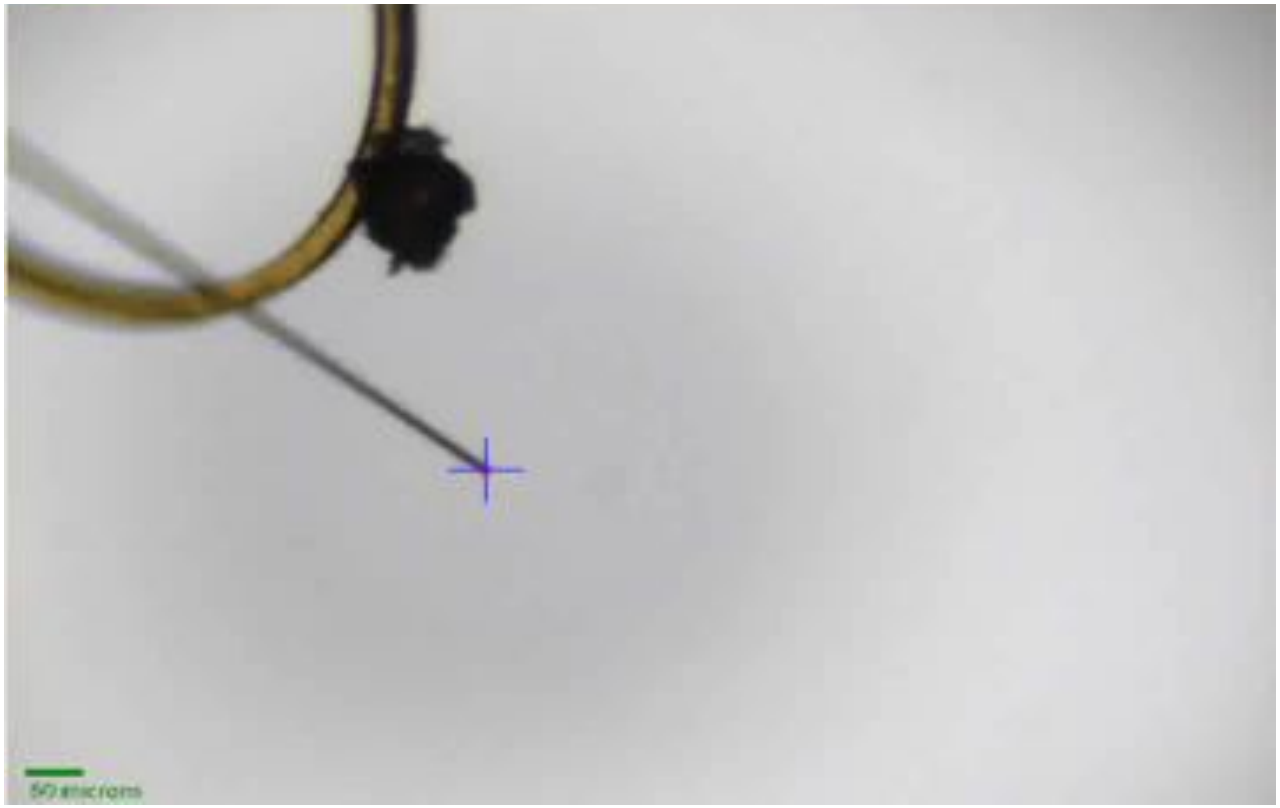

- Synchronous movement of omega, centring table and aligment table using direct PMAC programing to collect data along a long needle in a 'continuous helical scan'
- Here: carbon fibre 10 micron thick, 650 micron long.
- Real movement is smooth. Jumps are due to recording.

P14: 1D vs. 4D scan

- 'Monoclinic lysozyme' $P2_1$
  31.5 53.0 72.0 90 99.2 90.0
  70% solvent for 129 residues.
  crystal 150 x 15 x ?? µm
- 10 keV = 1.24 A
- half-focussed beam: 10 x 30 micron
- 1D: 0.2 deg / 0.04 sec, total = 36 secs.
  4D: 0.1 deg / 0.5 sec, total = 15 min.

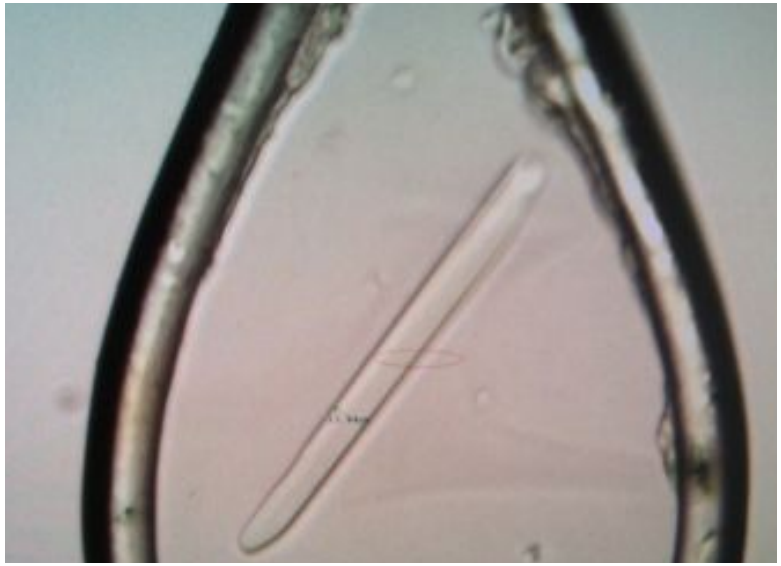

SUBSET OF INTENSITY DATA WITH SIGNAL/NOISE >= -3.0 AS FUNCTION OF RESOLUTION

RESOLUTION LIMIT	NUMBER OF REFLECTIONS OBSERVED	UNIQUE	POSSIBLE	COMPLETENESS OF DATA	R-FACTOR observed	R-FACTOR expected	COMPARED	I/SIGMA	R-meas	CC(1/2)	Anomal Corr	SigAno	Nano
6.83	1422	427	432	98.8%	5.3%	5.3%	418	18.34	6.4%	99.4*	-11	0.760	238
4.85	2375	723	747	96.8%	7.5%	7.8%	2367	12.69	9.0%	99.1*	-6	0.769	352
3.97	3216	922	938	98.3%	6.6%	6.7%	3207	15.37	7.9%	99.3*	4	0.830	488
3.44	3764	1098	1122	97.9%	8.0%	8.1%	3752	12.68	9.5%	99.1*	-9	0.709	540
3.08	4341	1245	1264	98.5%	12.1%	12.0%	4328	8.93	14.3%	98.1*	-5	0.804	597
2.81	4774	1371	1379	99.4%	19.4%	19.3%	4767	5.93	23.0%	94.8*	-9	0.761	635
2.60	5122	1484	1503	98.7%	25.1%	25.3%	5106	4.44	29.8%	92.7*	-1	0.777	674
2.43	5442	1583	1611	98.3%	32.9%	32.0%	5430	3.59	39.1%	87.8*	-2	0.796	656
2.29	5008	1559	1707	91.3%	43.5%	41.1%	4942	2.61	52.2%	81.9*	-8	0.760	535
total	35464	10412	10703	97.3%	13.2%	13.1%	35317	7.75	15.7%	98.7*	-5	0.775	4715

SUBSET OF INTENSITY DATA WITH SIGNAL/NOISE >= -3.0 AS FUNCTION OF RESOLUTION

RESOLUTION LIMIT	NUMBER OF REFLECTIONS OBSERVED	UNIQUE	POSSIBLE	COMPLETENESS OF DATA	R-FACTOR observed	R-FACTOR expected	COMPARED	I/SIGMA	R-meas	CC(1/2)	Anomal Corr	SigAno	Nano
4.77	3927	1208	1239	97.5%	4.0%	4.3%	3907	23.99	4.9%	99.5*	-17	0.701	576
3.38	7081	2107	2165	97.3%	4.3%	4.4%	7054	23.84	5.1%	99.6*	-16	0.744	964
2.76	9386	2737	2770	98.8%	5.7%	5.5%	9360	18.22	6.8%	99.4*	-15	0.763	1197
2.39	10840	3204	3272	97.9%	7.9%	7.8%	10799	13.02	9.4%	99.1*	-9	0.787	1285
2.14	12134	3623	3694	98.1%	11.6%	11.4%	12084	9.37	13.9%	98.1*	-4	0.784	1329
1.96	13387	3969	4078	97.3%	18.4%	19.1%	13328	6.03	21.9%	96.2*	-7	0.732	1404
1.81	14515	4346	4428	98.1%	35.3%	37.3%	14445	3.27	42.1%	88.9*	-9	0.682	1426
1.69	15419	4635	4725	98.1%	61.6%	66.7%	15338	1.89	73.5%	73.4*	-8	0.679	1430
1.60	10819	3945	5056	78.0%	82.1%	92.7%	10552	1.14	101.7%	52.5*	-9	0.645	791
total	97508	29774	31427	94.7%	8.3%	8.5%	96867	8.60	9.9%	99.6*	-9	0.728	10402

Microcrystal data collection

Ultralente Insulin in H3
a=b=80 Å c=37 Å
crystal: (3-5) x (3-5) x (5-10) μm^3
beam: 4x5 µm ('half'-focused)
exp: 1 s per 1° frame
~40 frames/crystal
Pilatus6MF

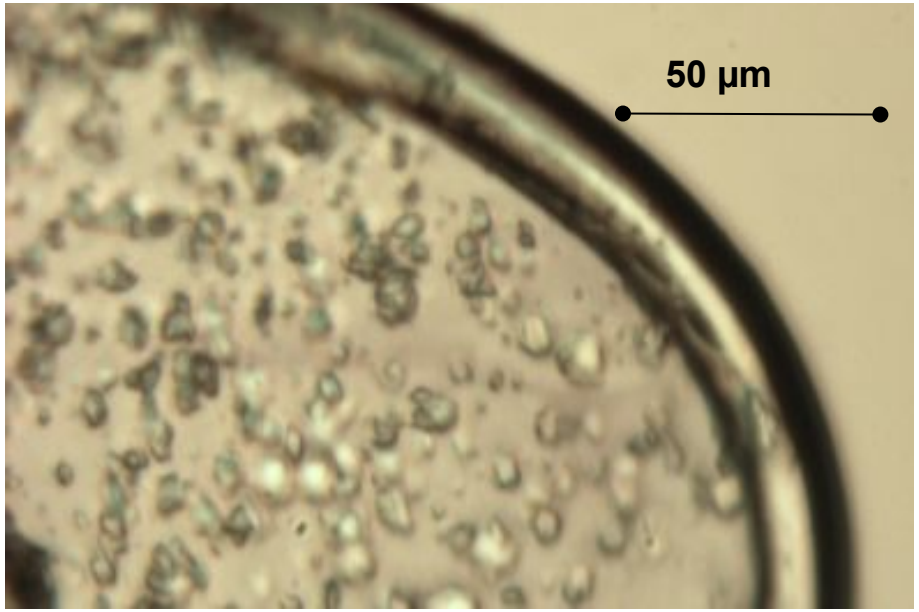

Partial data set statistics

SUBSET OF INTENSITY DATA WITH SIGNAL/NOISE >= -3.0 AS FUNCTION OF RESOLUTION

RESOLUTION LIMIT	NUMBER OF REFLECTIONS OBSERVED	UNIQUE	POSSIBLE	COMPLETENESS OF DATA	R-FACTOR observed	R-FACTOR expected	COMPARED	I/SIGMA	R-meas	CC(1/2)	Anomal Corr
8.34	86	78	168	46.4%	3.3%	3.3%	16	15.89	4.7%	99.6*	0
5.28	272	253	478	52.9%	4.5%	3.8%	38	13.53	6.4%	98.7*	0
3.93	540	496	960	51.7%	3.2%	3.6%	88	13.06	4.5%	99.4*	0
3.27	662	599	1154	51.9%	5.2%	5.1%	126	9.47	7.3%	99.1*	0
2.95	587	543	1012	53.7%	9.5%	8.7%	88	6.10	13.4%	97.8*	0
2.65	591	531	1420	37.4%	12.8%	12.7%	120	4.40	18.1%	97.0*	0
total	2738	2500	5192	48.2%	4.5%	4.5%	476	8.99	6.3%	99.5*	56

Ultralente insulin microcrystal structure solution

Isomorphous subset via cluster analysis

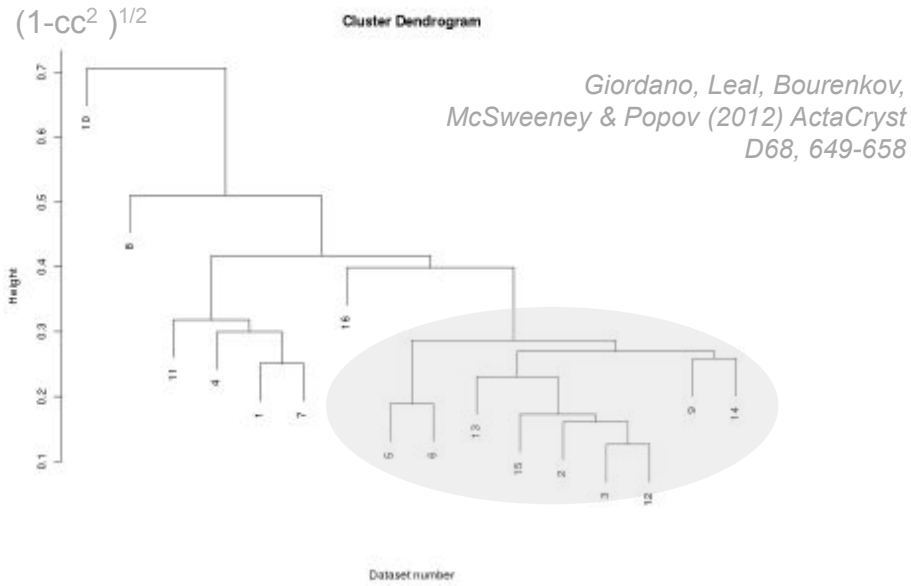

Giordano, Leal, Bourenkov, McSweeney & Popov (2012) ActaCryst D68, 649-658

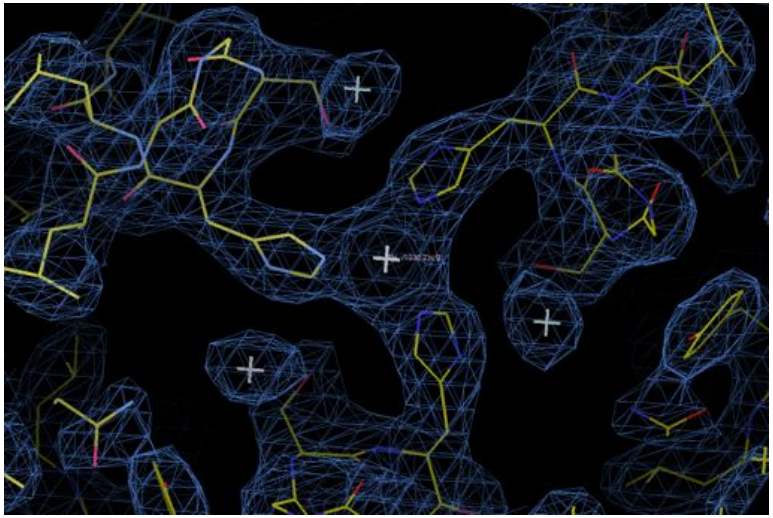

Electron density map, model phases
REFMAC R/Rfree=0.18/0.24

Combined data set statistics

SUBSET OF INTENSITY DATA WITH SIGNAL/NOISE >= -3.0 AS FUNCTION OF RESOLUTION

RESOLUTION LIMIT	NUMBER OF REFLECTIONS OBSERVED	UNIQUE	POSSIBLE	COMPLETENESS OF DATA	R-FACTOR observed	R-FACTOR expected	COMPARED	I/SIGMA	R-meas	CC(1/2)	Anomal Corr	SigAno	Nano
8.34	1989	168	168	100.0%	8.2%	9.3%	1987	25.91	8.6%	99.7*	61*	1.800	83
5.28	6054	486	486	100.0%	11.2%	11.5%	6053	21.13	11.7%	99.4*	52*	1.548	242
3.93	11427	964	964	100.0%	13.5%	12.5%	11424	19.50	14.1%	99.1*	30*	1.227	479
3.27	14393	1182	1182	100.0%	22.6%	21.8%	14393	12.74	23.6%	99.2*	16*	0.967	591
2.95	12132	987	988	99.9%	43.8%	48.5%	12132	7.79	45.7%	97.5*	14	0.840	493
2.65	12892	1341	1442	93.0%	68.5%	82.9%	12822	4.28	72.0%	89.8*	-2	0.708	617
total	58887	5128	5230	98.0%	17.4%	17.7%	58811	12.07	18.1%	99.5*	23*	1.012	2505

Refinement

A 'good' model should …

- Agree with the data

$$R = \frac{\sum_{hkl} \left| F_{hkl}^{obs} - F_{hkl}^{calc} \right|}{\sum_{hkl} \left| F_{hkl}^{obs} \right|}$$

- Agree with what we know

EMBL

Progress of a Refinement

#par is number of parameter in model
#obs is number of reflections used in refinement
Rw is Rwork in percent
Rf is Rfree in percent
Rd is the difference betwee Rw and Rf in percent
CPU is approximate CPU time [secs] normalized to a Pentium III running at 500 MHz

step	data used	#par	#obs	Rw	Rf	Rd	CPU
molecular replacement	15.0-4.0	3	775	44.5	-	-	30
rigid body	10.0-2.5	9	2997	46.4	47.4	1.0	140
first round	10.0-1.5	3887	13818	30.2	34.3	4.1	500
after first rebuild 10cgls	"	3735	"	26.2	31.4	5.2	360
SHELXWAT	"	4091	"	20.2	24.6	4.4	2000
bld + SHELXWAT	"	4231	"	18.7	22.8	4.1	2000
include all data 20cgls	10.0-1.1	4203	33993	19.1	21.7	2.6	1450
ANIS 20cgls	"	9453	"	16.0	19.2	3.2	2850
Rebuild 10 SHELXWAT	"	9557	"	13.4	15.8	1.8	1480
rebuild 10 cgls	"	10481	"	12.3	15.3	3.0	1610
rebuild 10 cgls	"	10819	"	12.1	15.1	3.0	1650
rebuild 10 cgls	"	10838	"	11.6	14.6	3.0	1800
rebuild 10 cgls	"	11494	"	11.3	14.4	3.1	1800
rebuild 10 cgls	"	11576	"	11.0	14.0	3.0	1800
rebuild 10 cgls	"	11774	"	10.7	13.8	3.1	1800
put hydrogens	10.0-1.1	11765	"	9.7	12.8	3.1	2500
include test set	10.0-1.1	11693	35786	9.8	-	-	2600

EMBL

Target Function

- Implements our idea of agreement between the data and the measurements. One possible form is:

$$E_{X-ray} = \sum_{hkl} \left| F_{hkl}^{obs} - k\, F_{hkl}^{calc} \right|^2$$

- One could replace F_{obs} by I_{obs}.
- The *hkl*-terms can be weighted by the uncertainties of the measurements: $1/\sigma(F_{obs})$.
- Other functions, such as the $CC(F_{obs},F_{calc})$, can be used.

EMBL

Observables and Parameters

res	#r/a	parameters	d:p
3.0	2	x y z	0.6:1
2.5	4	x y z B?	1:1
2.0	8	x y z B	2:1
1.5	20	x y z B	5:1
1.1	50	x y z U_{11} U_{22} U_{33} U_{12} U_{13} U_{23}	5:1
0.9	90	x y z U_{11} U_{22} U_{33} U_{12} U_{13} U_{23}	10:1

Numbers are for a protein crystal with 40% solvent. Lysozyme (129 amino acids 1001 atoms) will produce ca. 32000 reflections to 2 Å resolution.

EMBL

Stereochemical Restraints

Acta Cryst. (1991). A47, 392–400

Accurate Bond and Angle Parameters for X-ray Protein Structure Refinement

By Richard A. Engh and Robert Huber

Max Planck Institut für Biochemie, D8033 Martinsried bei München, Germany

Table 1. *CSD parametrization atom types*

Atom type	Description
C	Carbonyl C atom of the peptide backbone
C5W*	Tryptophan C^{γ}
CW*	Tryptophan $C^{\delta 2}$, $C^{\epsilon 2}$
CF*	Phenylalanine C^{γ}
CY*	Tyrosine C^{γ}
CY2*	Tyrosine C^{ϵ}
C5*	Histidine C^{γ}
CN*	Neutral carboxylic acid group C atom
CH1E	Tetrahedral C atom with one H atom
CH2E	Tetrahedral C atom with two H atoms (except CH2P, CH2G)
CH2P*	Proline C^{γ}, C^{δ}
CH2G*	Glycine C^{α}
CH3E	Tetrahedral C atom with three H atoms
CR1E	Aromatic ring C atom with one H atom (except CR1W, CRH, CRHH, CR1H)
CR1W*	Tryptophan $C^{\zeta 2}$, $C^{\eta 2}$
CRH*	Neutral histidine $C^{\epsilon 1}$
CRHH*	Charged histidine $C^{\epsilon 1}$
CR1H*	Charged histidine $C^{\delta 2}$
N	Peptide N atom of proline
NR	Unprotonated N atom in histidine
NP	Pyrrole N atom
NH1	Singly protonated N atom (His, Trp, peptide)
NH2	Doubly protonated N atom
NH3	Triply protonated N atom
NC2	Arginine $N^{\eta 1}$, $N^{\eta 2}$
O	Carbonyl O atom
OC	Carboxyl O atom
OH1	Hydroxyl O atom
S	S atom
SM*	Methionine S atom
SH1E	Singly protonated S atom

* Atom types marked with an asterisk are new (non-*XPLOR*) types.

Table 2. *Bond parameters*

Bond type	σ	Bond length (Å)
C5W–CW	0·018	1·433
CW–CW	0·017	1·409
C–CH1E	0·021	1·525
C5–CH2E	0·014	1·497
C5W–CH2E	0·031	1·498
CF–CH2E	0·023	1·502
CY–CH2E	0·022	1·512
C–CH2E		
CN–CH2E		
C–CH2G		
C5W–CR1E		
CW–CR1E		
CW–CR1W		
CF–CR1E		
CY–CR1E		
CY2–CR1E		
C5–CR1H		
C5–CR1E		
C–N		
C–NC2		
C5–NH1		
CW–NH1		

Table 3. *Angle parameters*

Angle type	σ	Angle (°)	Angle t
C5W–CW–CW	1·2	107·2	CH3E–C
CW–C5W–CH2E	1·4	126·8	CH3E–C
C5W–CW–CR1E	1·0	133·9	CH3E–C
CW–CW–CR1E	1·0	118·8	C–CH2E
CW–CW–CR1W	1·0	122·4	C5–CH2
CW–C5W–CR1E	1·6	106·3	CF–CH2
CW–CW–NH1	1·3	107·4	C5W–CH
CH1E–C–N	1·5	116·9	CY–CH2
CH1E–C–NH1	2·0	116·2	C–CH2E
CH1E–C–O	1·7	120·8	C–CH2G
CH1E–C–OC	2·5	117·0	C–CH2G
CH2E–C5–CR1E	1·3	129·1	CH1E–C
CH2E–C5–CR1H	1·3	131·2	CH1E–C
CH2E–CF–CR1E	1·7	120·7	CH1E–C
CH2E–C5W–CR1E	1·5	126·9	CH1E–C
CH2E–CY–CR1E	1·5	120·8	CH1E–C
CH2E–C–N	[illegible]	[illegible]	CH1E–C

Bond lengths and angles should be consistent with these values ('Engh&Huber Dictionary') derived from small molecule structures. ITC-F contains an updated version (§18.3).

EMBL

Enforcing stereochemistry

$$E_{bond} = \sum_{bonds} \frac{\left| d^{obs} - d^{EH} \right|^2}{\sigma_{d^{EH}}}$$

- E_{bond} is zero for a perfect agreement between expected bond lengths and bond lengths measured in the model. The value of E_{bond} increases for increasing deviations.
- The weight for each bond-type depends on the spread observed in small molecule structures

EMBL

Enforcing stereochemistry

- Target functions can be defined for various geometrical properties:

$$E_a = \sum_a \frac{\left| a^{obs} - a^{ex} \right|^2}{\sigma_{a^{ex}}}$$

- And combined into an overall function:

$$E_{chem} = E_{bond} + E_{angle} + E_{chir} + \ldots$$

EMBL

Combined Target Function

$$E_{tot} = E_{chem} + w_{X-ray} E_{X-ray}$$

- E_{chem} contains information about bond-lengths, -angles, planarity, chirality, non-bonded repulsion, electrostatic interactions etc. (the *a priori* knowledge).
- $w_{X\text{-}ray}$ is the relative weight between chemical information and experimental data. It depends not only the amount of data but also on the quality of the data.

EMBL

Optimization of the Target Function

$$E_{tot} = E_{chem} + w_{X-ray} E_{X-ray}$$

- Minimization of E_{tot} should deliver a model that (1) is consistent with the data and (2) has reasonable stereochemistry.
- At 2 Å, 5000 atoms correspond to ca. 20000 parameters to be refined against 50000 reflections.

The multiple minima problem

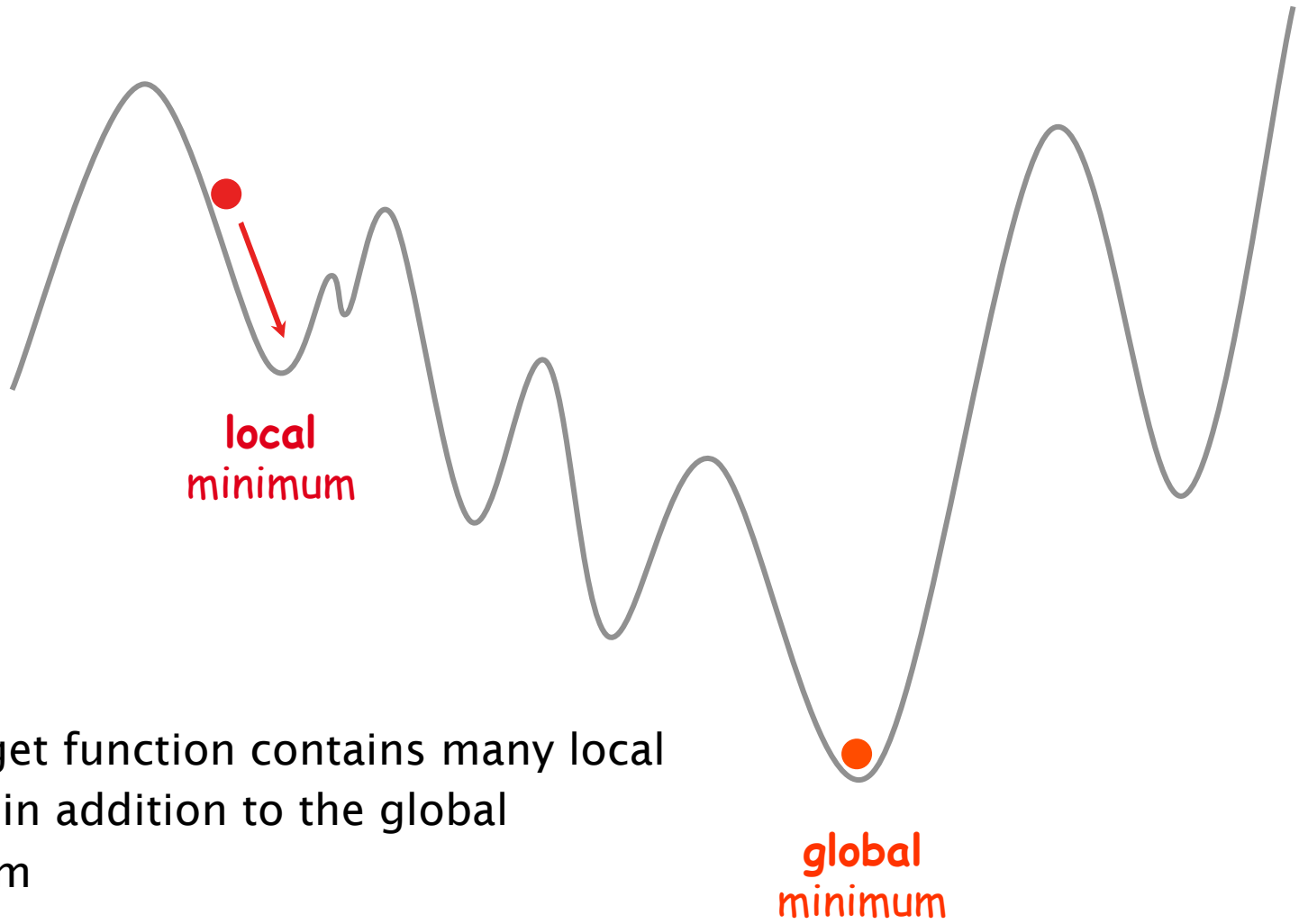

- The target function contains many local minima in addition to the global minimum
- Standard minimizers will reach the 'closest' local minimum but not the global minimum

EMBL

Getting out of Local Minima

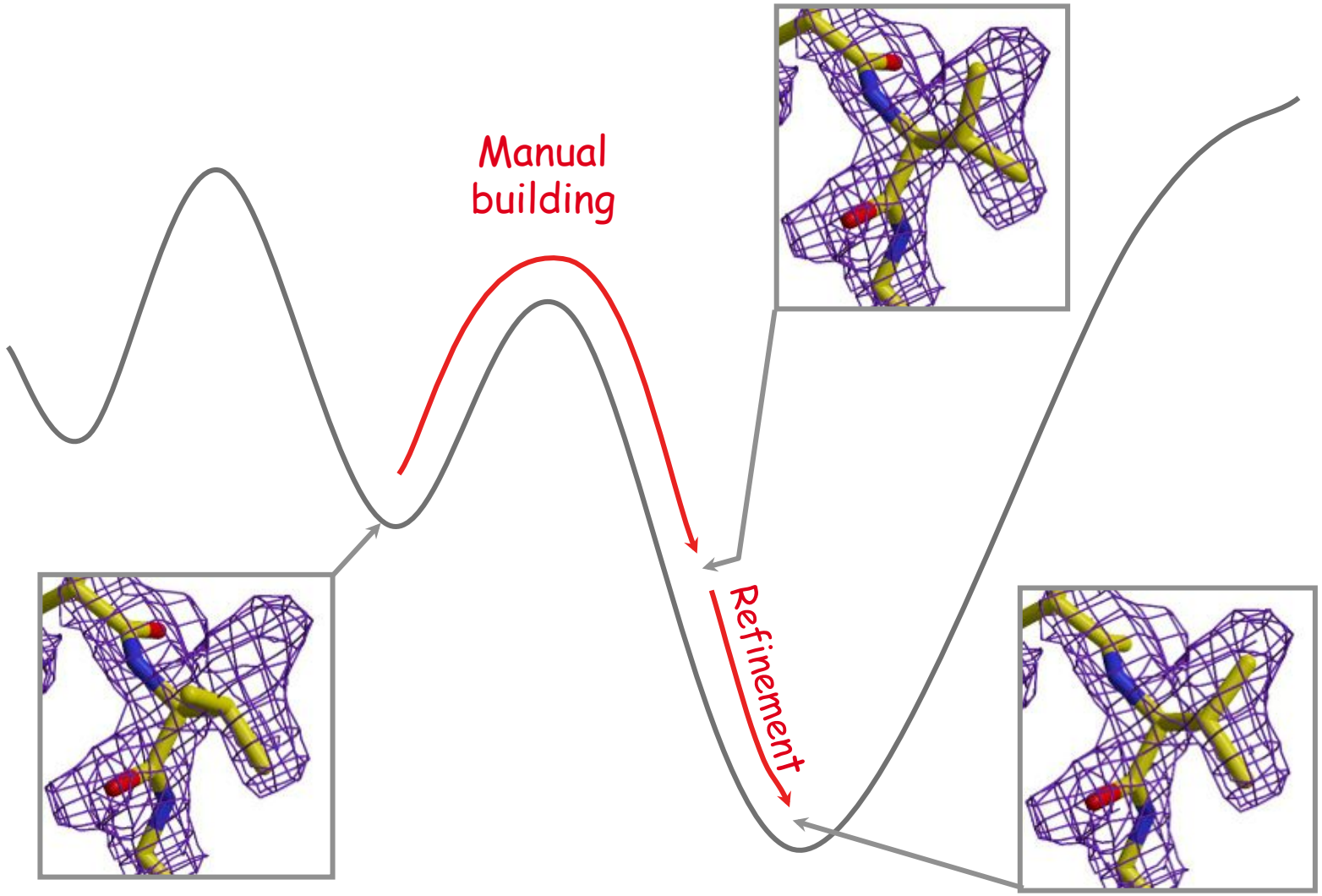

EMBL

Simulated Annealing

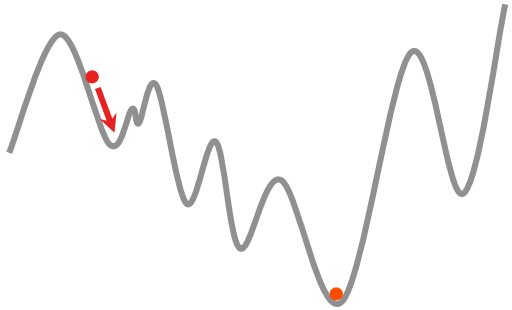

- A method to search conformational space
- *Annealing is a physical process wherein a solid is heated so that the particals assume random positions and then is cooled slowly so that all particles can arrange into their lowest energy state.*
- The target function E can be considered as the potential energy of the system and then a molecular dynamics simulation is run (in fact, historically, XPLOR (later CNS, later PHENIX) was an MD-program with an additional energy term $E_{X\text{-}ray}$).

EMBL

Simulated Annealing

Figure from
Paul Adam's lecture notes

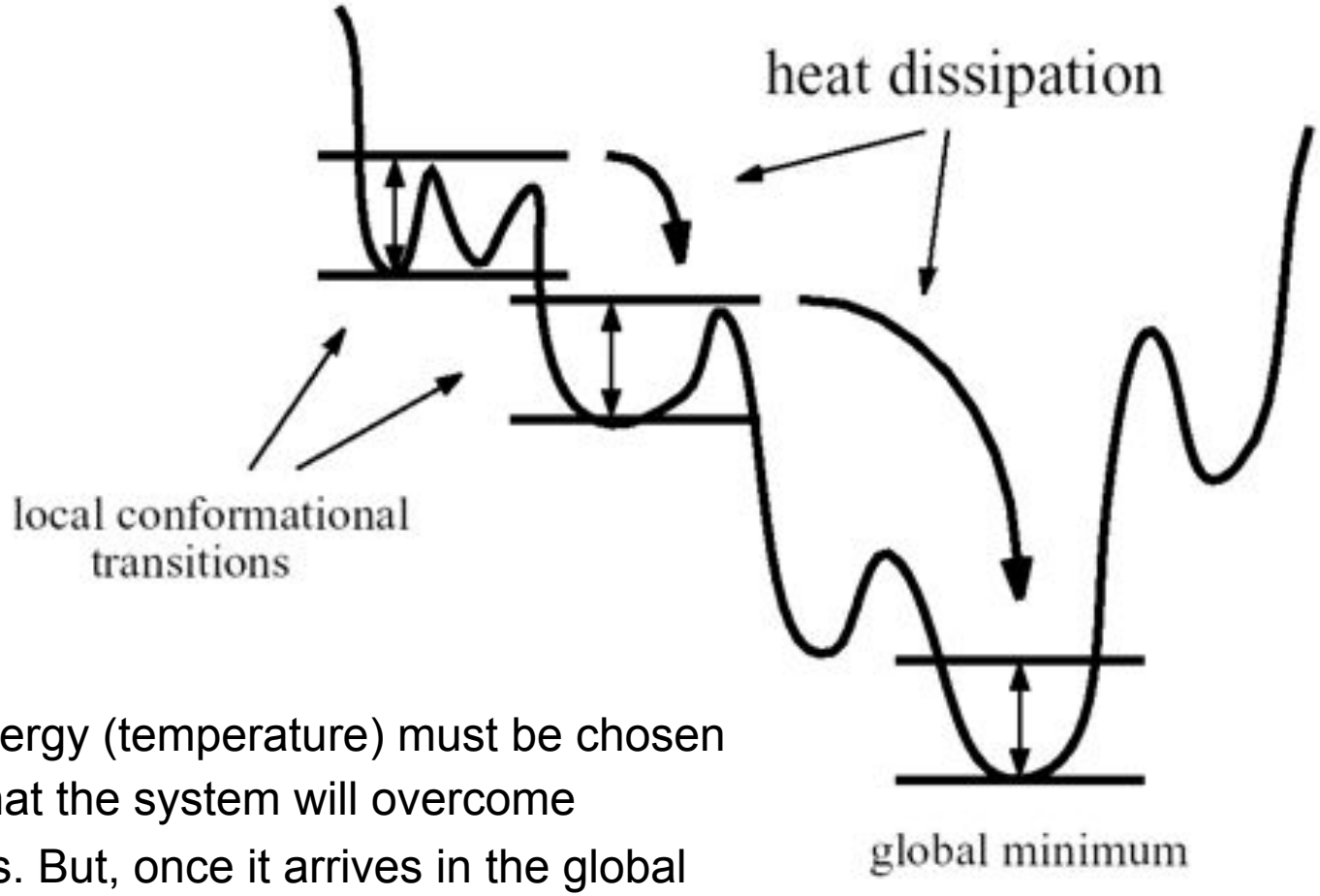

The energy (temperature) must be chosen such that the system will overcome barriers. But, once it arrives in the global minimum, it should not escape from there.

Observables and Parameters

res	#r/a	parameters	d:p
3.0	2	x y z	0.6:1
2.5	4	x y z B?	1:1
2.0	8	x y z B	2:1
1.5	20	x y z B	5:1
1.1	50	x y z U_{11} U_{22} U_{33} U_{12} U_{13} U_{23}	5:1
0.9	90	x y z U_{11} U_{22} U_{33} U_{12} U_{13} U_{23}	10:1

Constraints

- Constraints couple parameters to each other such that the overall number of parameters is reduced.
- Segmented rigid bodies
  - Entire residues
  - Rigid groups (guanodinio, carboxylate, aromatic rings)
  - Entire domains

Torsion Angle Refinement

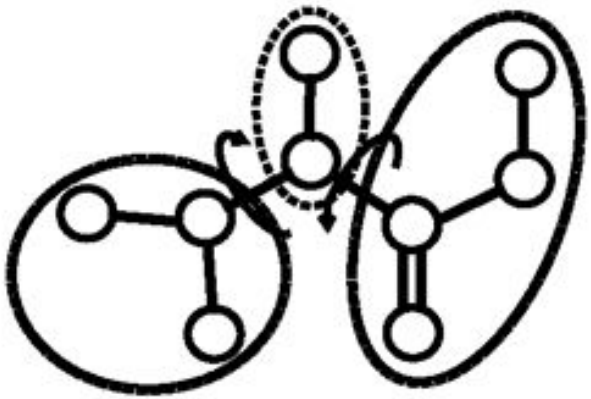

- Deviations in bond lengths and angles are usually small.
- Torsion angles can be used as 'normal coordinates of protein dynamics'
- This reduces the number of parameters dramatically (up to a factor of 10)
- Initially introduced by Diamond (1971); implemented in XPLOR by Rice & Brunger (1996).
- Large radius of convergence (e.g. for bad molecular replacement models).

Diamond (1971) Acta Cryst. A27:436-452
Sussmann (1977) Acta Cryst. A33:800
Rice & Brunger (1996) Proteins 19:277-290

B-factors

- A ‘crystal structure’ represents a space and time average (many molecules in the crystal for the time of the experiment).
- The coordinates of an atom in the pdb-file represent the mean coordinates. The spread around the mean coordinates is described by the B-factor.
- Some Examples:

$B = 5\ Å^2$	$\langle u \rangle = 0.25\ Å$
$B = 20\ Å^2$	$\langle u \rangle = 0.50\ Å$
$B = 40\ Å^2$	$\langle u \rangle = 0.71\ Å$
$B = 80\ Å^2$	$\langle u \rangle = 1.01\ Å$

- A typical bondlength is 1.5 Å !

$$B = 8\pi^2\langle u^2 \rangle,$$

where $\langle u^2 \rangle$ is the mean square displacement

B-factors

- Low
  - In well ordered region
- High
  - In loops
  - On the surface
  - In terminal regions

- Here
  - Red is high
  - Blue is low

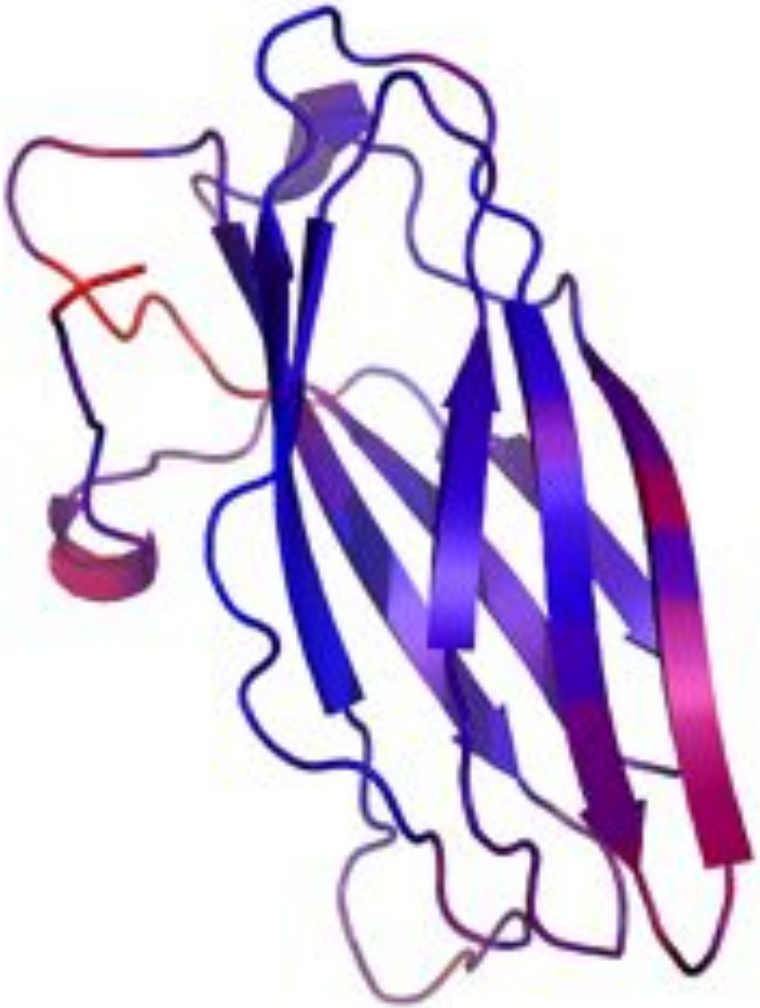

EMBL

B-factors and electron density

All pictures were taken from the same structure refined at 2.0 Å resolution.
Countoured at the same level

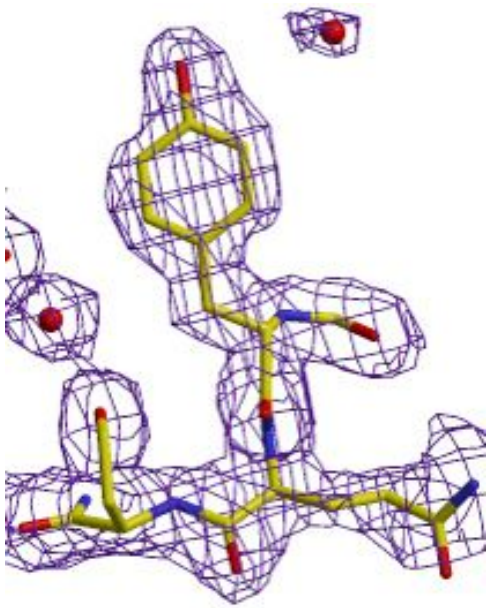

Tyr48
B = 20.9 Å^2
RSR = 0.12

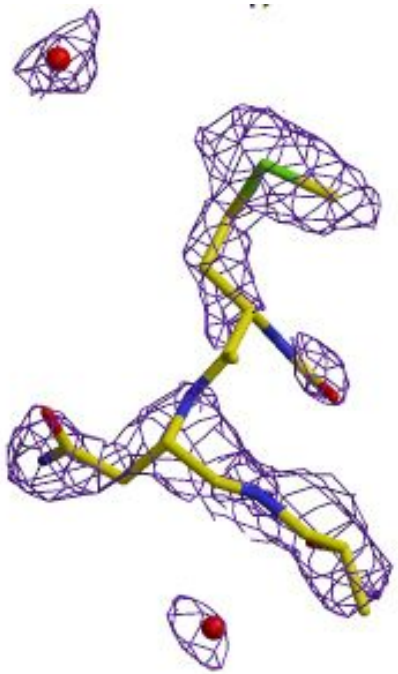

Met285/Asn286
B = 69.9 Å^2 / 69.1 Å^2
RSR = 0.25 / 0.18

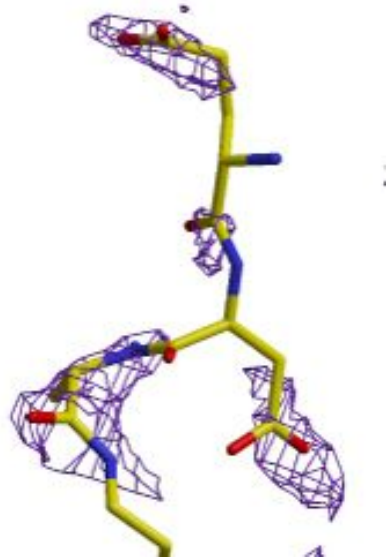

Glu229/Asp230
B = 73.9 Å^2 / 73.4 Å^2
RSR = 0.39 / 0.27

EMBL

Serial Femto-second crystallography

- X-ray Free Electron Lasers (LCLS Stanford, SACLA Harima, EU-XFEL Hamburg) deliver 10^{12}-10^{13} photons in a pulse of 50-100 fsec duration. (1 fsec = 10^{-12} sec)
- 1 XFEL pulse contains ca. the number of monochromatic photons a synchrotron can deliver in 1 sec.
- Such a pulse carries enough energy to convert anything in its way into plasma.
- Can we use XFEL radiation for macromolecular crystallography?

Consider a molecular in an XFEL-puls

Diffraction before Destruction

Neutze, R., Wouts, R., van der Spoel, D., Weckert, E., & Hajdu, J. (2000). Potential for biomolecular imaging with femtosecond X-ray pulses. *Nature*, *406*(6797), 752–757. doi:10.1038/35021099

Experimental Setup

http://kenandrachel.com/wp-content/uploads/2012/04/Selection_003.png

Photosystem I (8.5 Å)

3/2/2011 Chapman, H. N., Fromme, P., Barty, A., White, T. A., Kirian, R. A., Aquila, A., et al. (2011). Femtosecond X-ray protein nanocrystallography. *Nature*, *470*(7332), 73–77. doi:10.1038/nature09750

Photosystem I

3/2/2011 Chapman, H. N., Fromme, P., Barty, A., White, T. A., Kirian, R. A., Aquila, A., et al. (2011). Femtosecond X-ray protein nanocrystallography. *Nature*, *470*(7332), 73–77. doi:10.1038/nature09750

- Resolution limited due to low energy / long wavelength

Lysozyme (1.9 Å)

20/7/2012 Boutet, S., Lomb, L., Williams, G. J., Barends, T. R. M., Aquila, A., Doak, R. B., et al. (2012). High-Resolution Protein Structure Determination by Serial Femtosecond Crystallography. *Science (New York, NY)*. doi:10.1126/science.1217737

- Shorter wavelength

Lysozyme (1.9 Å)

20/7/2012 Boutet, S., Lomb, L., Williams, G. J., Barends, T. R. M., Aquila, A., Doak, R. B., et al. (2012). High-Resolution Protein Structure Determination by Serial Femtosecond Crystallography. *Science (New York, NY)*. doi:10.1126/science.1217737

Cathepsin B

Koopmann, R., Cupelli, K., Redecke, L., Nass, K., Deponte, D. P., White, T. A., et al. (2012). In vivo protein crystallization opens new routes in structural biology. Nature Methods, 9(3), 259–262. doi: 10.1038/nmeth.1859